

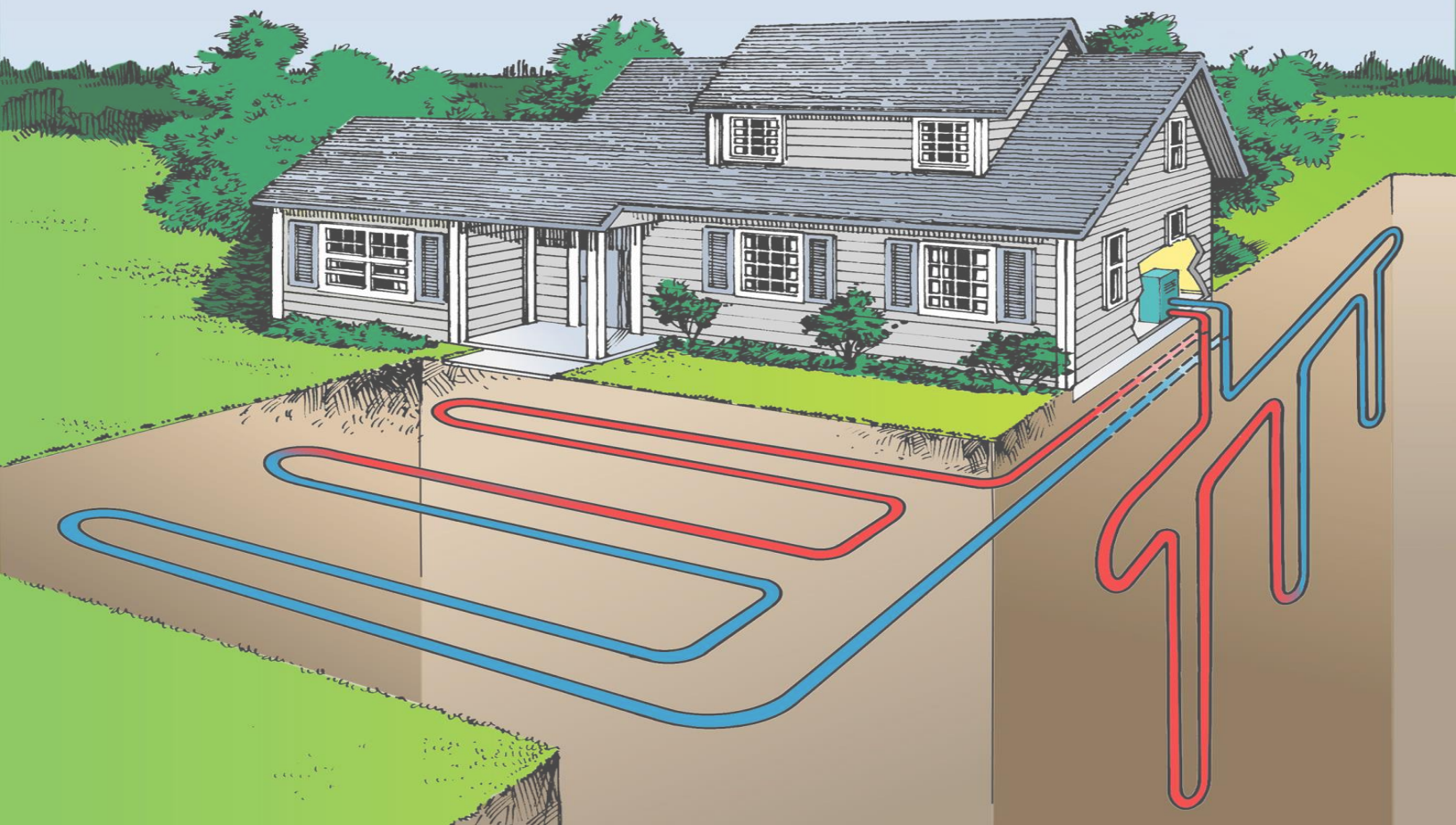
# **Assessment of the effect of groundwater flow on the performance of Borehole Thermal Energy Storage systems**

**Nefeli M. Panteli**

Delft University of Technology

Faculty of Civil Engineering and Geosciences

Department of Water Management





# **Assessment of the effect of groundwater flow on the performance of Borehole Thermal Energy Storage systems**

by

**Nefeli – Myrsini Panteli**

in partial fulfilment of the requirements for the degree of

**Master of Science**  
in Water Management

at the Delft University of Technology,  
to be defended publicly on Monday June 11, 2018

Supervisor:	Prof.dr.ir. Mark Bakker, TU Delft
Thesis committee:	Ir. Martin Bloemendaal, TU Delft
	Ir. Bas des Tombe, TU Delft
	Dr. PJ (Phil) Vardon, TU Delft
	Ir. Henk Witte, Groenholland BV
	Ir. Frank de Winkel, Itho – Daalderop



## Acknowledgements

I would like to thank all the members of my committee; Mark Bakker and Phil Vardon, for their useful input and feedback; Henk Witte from Groenholland, for offering his valuable experience and ideas; Frank de Winkel from Itho-Daalderop, for providing all the data that was necessary to carry out this project. I would like to especially thank my daily supervisors, Martin Bloemendaal and Bas des Tombe, for their continuous help, offering inspiration and excellent guidance. I would also like to thank my family, for their support and encouragement during my studies, and all my friends that have shared this experience with me and supported me throughout my thesis.



## **Abstract**

In a Borehole Thermal Energy Storage (BTES) system, heat is extracted from or injected to the subsurface, taking advantage of the relatively constant temperatures of the underground. Both thermal conduction and advection can influence the performance of BTES systems, but thermal advection is often neglected in the design process. However, in areas with groundwater flow, the heat exchange between the BTES system and the soil can be significantly affected, as the stored heat is transported from the borehole with the flow. This project studies the influence of groundwater flow on the performance of a BTES system. A detailed 3D numerical model is created using MODFLOW and MT3D to simulate groundwater flow and heat transfer under various conditions. The model is verified using an analytical solution as well as experimental data, and is subsequently used to perform a sensitivity analysis and simulate a case study, in order to gain insight on the influence of groundwater flow on the heat exchange process and the conditions that favor this effect. The results reveal that groundwater flow is enhancing the heat exchange rates both in heating and in cooling mode. The magnitude of the effect depends on the total groundwater discharge, and the porosity and background temperature of the soil. In cases of combined heating and cooling, the effect also depends on the magnitude and ratio of the injected and extracted energy loads, as well as the frequency of switching between storage and extraction. Finally, it is revealed that groundwater flow is beneficial for systems with unbalanced energy loads, as it counterbalances the net heat extraction or injection that could decrease the system's heat exchange capacity in the long term.



## Preface

Groenholland BV is one of the leading companies in the development and implementation of geothermal energy storage systems in the Netherlands. Their activities range from TRT testing & data analysis to the design, engineering and implementation of geothermal heat pump installations. Groenholland has been involved in over 250 shallow geothermal projects that vary in size from private estates to large public and commercial buildings or even large scale housing development. Other activities include participation in a number of EU research projects, active membership of National and International bodies, teaching and development of energy plans or specific guidelines and legislation related to shallow geothermal energy for National and local government. Groenholland has performed extensive research in the field of borehole heat exchange; in cooperation with TU Delft, they aim to further investigate the effect of groundwater flow on the performance of BTES systems.

Itho-Daalderop is a Dutch company that specializes in domestic heating products works under the slogan *Climate for Life*. They are actively contributing to the 2020 Energy Strategy set by the EU by taking part in the development of energy-neutral buildings. Itho-Daalderop has installed over 80.000 geothermal heat pump systems in the Netherlands and every heat pump is equipped with an integrated monitoring device from which performance data is collected. The case study presented in this project is using data provided by Itho-Daalderop.



## Table of contents

Assessment of the effect of groundwater flow on the performance of Borehole Thermal Energy Storage systems .....	
Acknowledgements .....	i
Abstract.....	iii
Preface .....	v
Table of contents .....	vii
Table of figures .....	ix
1. Introduction .....	1
1.1. BTES and groundwater flow.....	1
1.2. Previous research.....	3
1.3. Scope and approach.....	4
2. Developing simulation method to model the effect of groundwater flow on BTES systems.....	6
2.1. Description of simulated area and assumptions .....	6
2.2. Description of the models.....	8
2.2.1. Analytical “line-source” model .....	8
2.2.2. Numerical “cable” model (2D) .....	9
2.2.3. Numerical “pipe” model (3D).....	13
2.3. Results.....	15
3. Main BTES model .....	18
3.1. Description .....	18
3.2. Results.....	20
3.3. Verification of model .....	24
3.4. Sensitivity analysis .....	25
3.4.1. Scenarios .....	25
3.4.2. Output parameters .....	27
3.4.3. Results.....	28
3.5. Conclusions .....	43
4. Case study .....	45
4.1. Description of BTES system.....	45
4.2. Implementation of recorded dataset to the model.....	47
4.3. Scenarios .....	48

4.4. Discussion.....	53
5. Conclusions and recommendations.....	54
5.1. Conclusions and further research suggestions .....	54
5.2. Suggestions for model improvement.....	55
References .....	57

## Table of figures

Figure 1: Different types of geothermal energy systems (Source: BodemenergieNL) .....	1
Figure 2: Closed vertical heating & cooling (BTES) systems. (Source: Soilpedia) .....	2
Figure 3: Main processes of heat transfer in the subsurface .....	3
Figure 4: Top view of grid, boundaries and heads of the 2D numerical “cable” model.....	10
Figure 5: Schematization of a cross-section of the 3D numerical “pipe” model.....	14
Figure 6: Distribution of the temperature increase in the soil around the heat source at the end of the 60 day period.....	15
Figure 7: Distribution of temperature increase in the soil along cross sections crossing the heat source. Comparison between the 3 models at the end of the 60 day period.....	16
Figure 8: Differences between the distributions of temperature increase of Figure 7.....	16
Figure 9: Relative errors (%) between the distributions of temperature increase of Figure 7. ....	17
Figure 10: Horizontal cross-section of grid and boundaries of the main 3D BTES model (top layer) .....	18
Figure 11: Schematization (top view and cross section) of the BTES system and its properties as simulated in the 3D model.....	19
Figure 12: Distribution of temperature increase at different time steps in the soil layer around the bottom of the borehole.....	21
Figure 13: Distribution of temperature increase in the soil along a cross section crossing the bottom of the BTES system, in the direction of the flow, for different time steps.....	22
Figure 14: Distribution of temperature decrease in the pipe, for different time steps .....	23
Figure 15: Cumulative energy flux rate absorbed by the soil for each point along the pipe .....	23
Figure 16: Average temperatures of fluid in BTES system. Comparison of modeled and measured temperatures for the reference experiment (A) and the experiment with groundwater flow (B).....	25
Figure 17: Configuration of pipes in scenarios 0 and E.....	26
Figure 18: Comparison of the distribution of soil temperature increase for different levels of groundwater discharge (GWF).....	29
Figure 19: Comparison of the distribution of temperature decrease in the pipe for different levels of groundwater discharge (GWF) .....	30

Figure 20: Comparison of the distribution of soil temperature increase for different levels of pipe flow velocity ( $u$ ) .....	31
Figure 21: Comparison of the distribution of temperature decrease in the pipe for different levels of pipe flow velocity ( $u$ ) .....	32
Figure 22: Comparison of the distribution of soil temperature increase for different values of porosity ( $n$ ).....	33
Figure 23: Comparison of the distribution of temperature decrease in the pipe for different values of porosity ( $n$ ).. .....	34
Figure 24: Comparison of the distribution of soil temperature increase for different values of background soil temperature. ....	35
Figure 25: Comparison of the distribution of temperature decrease in the pipe for different levels of background soil temperature .....	36
Figure 26: Relationship between output temperature difference of the pipe and background soil temperature.....	36
Figure 27: Comparison of the distribution of soil temperature increase for different configurations of the BTES system. ....	38
Figure 28: Comparison of the distribution of temperature decrease in the pipe for different configurations of the BTES pipe.....	38
Figure 29: Comparison of the distribution of temperature decrease in the pipe for cases of groundwater flow in different soil layers.. .....	39
Figure 30: Distribution of temperature change in the soil on a horizontal cross-section around the bottom of the borehole, after 25 years of constant operation of the systems. A: Scenario 0 (single BTES system). B: Scenario G: Two BTES systems placed at a distance of 10m from each other.....	41
Figure 31: Comparison of the distribution of soil temperature increase in case of one or two BTES systems.....	42
Figure 32: Comparison of the distribution of temperature decrease in the pipe in case of one or two BTES systems in the area .....	42
Figure 33: Location of the BTES case study system .....	45
Figure 34: Isohypses map of the area around Bakel.....	47
Figure 35: Comparison of modeled and measured output temperatures and input temperatures of the BTES case study system.....	48

Figure 36: Illustration of the heating - cooling demand profile.....	50
Figure 37: Temperature differences between output and input of the BTES pipe, with and without groundwater flow.....	51
Figure 38: Heat transfer rates of the BTES system, with and without groundwater flow.....	51
Figure 39: Temperatures of the soil at selected points, located 30 m deep, with and without groundwater flow. ....	52



# 1. Introduction

## 1.1. BTES and groundwater flow

Geothermal energy is energy generated by or stored in the earth. It is widely used for the heating and cooling of buildings, as it is a highly efficient, reliable and sustainable technology that significantly contributes to the reduction of greenhouse gas emissions, according to the targets set by the EU (Chiasson et al., 2000; Richards, 2017).

As depicted in Figure 1, geothermal energy systems can be categorized in shallow and deep. Shallow installations are considered as not exceeding a depth of 400 m and (natural) geothermal source temperatures of 25 °C (Bakema & Schoof, 2016), while deep installations use higher temperatures and can be installed at depths up to 5 km (REA - Renewable Energy Association). Geothermal systems can also be distinguished between open systems (Aquifer Thermal Energy Storage – ATES), which can be either shallow or deep, and closed systems (Borehole Thermal Energy Storage – BTES), which are shallow (usually reaching up to 200 m of depth).

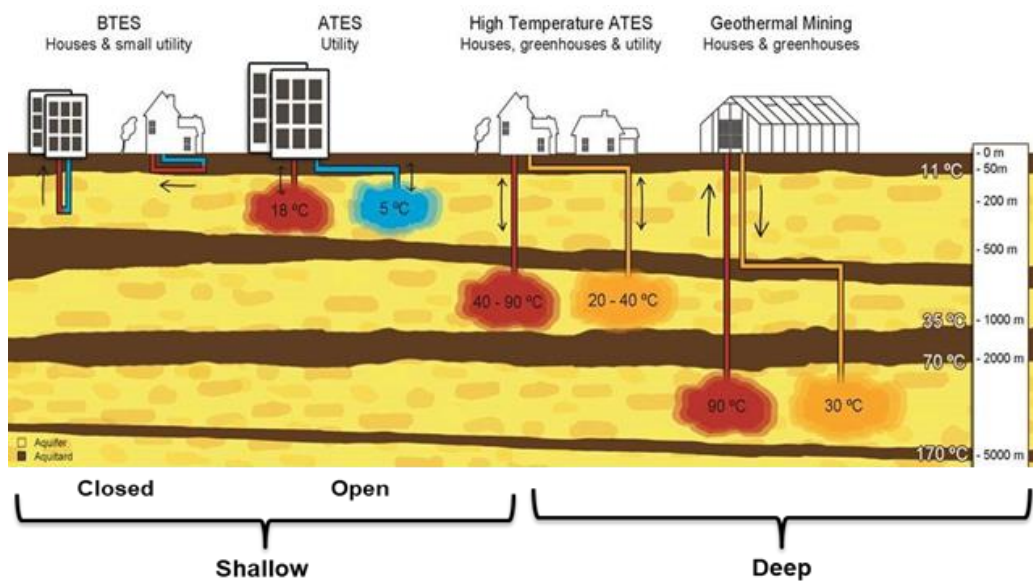
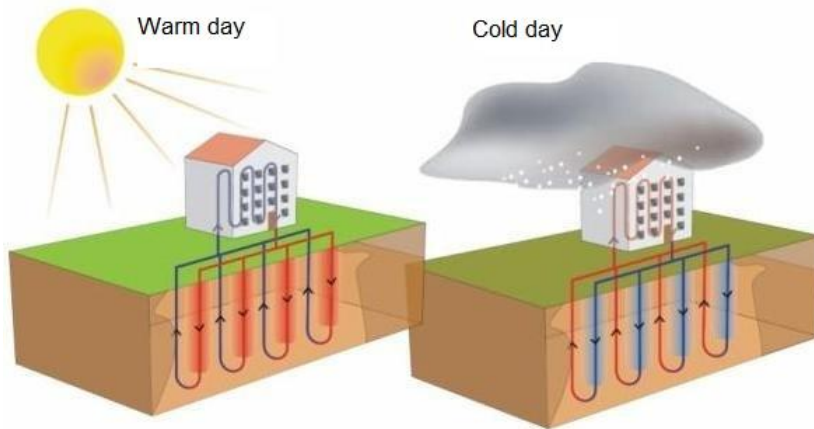


Figure 1: Different types of geothermal energy systems (Source: BodemenergieNL)

BTES systems, which are the subject of this project, are the most common type of thermal energy storage, and they are becoming increasingly popular: there are currently more than 50.000 BTES installations in the Netherlands (Bakema & Schoof, 2016). Generally, BTES systems are used to store energy, which means that the annual thermal load is nearly balanced – as opposed to ordinary Borehole Heat Exchangers (BHE), which are used for either heating or cooling (Banks, 2012). In the Netherlands, most systems are used for both heating and cooling, therefore the term BTES will be used for the rest of the report.

Opposite to ATES , where water is extracted and injected directly into the aquifer, BTES systems consist of pipes that form closed loops: energy is exchanged with the subsurface by means of a fluid (water or an antifreeze formulation such as glycol) circulating through the pipes that are buried in the ground. The pipes can be placed horizontally or, more commonly, vertically in the ground, forming one or multiple loops. The depth of the borehole usually ranges between 40–150 m (Diao et al., 2004). Taking advantage of the relatively stable underground temperatures, the fluid exchanges heat with the ground around the borehole – heat is stored or extracted depending on the needs of the building (heating or cooling). Figure 2 shows an illustration of this process.



**Figure 2: Closed vertical heating & cooling (BTES) systems. (Source: Soilpedia)**

The energy gained by BTES systems is usually applied in combination with a Ground Source Heat Pump (GSHP). After the carrier fluid has been transported through the pipes, it gains a temperature difference of about 3 – 4 °C, which is not enough to heat or cool a building. However, this small temperature difference gained over a large volume of water corresponds to a sufficient energy input for the compressional heat pump, which compresses the fluid to generate the desired temperatures. These systems have a high thermal efficiency, which is defined as the ratio of net heat output (in heating mode) or heat removal (in cooling mode), to the energy input. They are even more efficient compared to conventional Air Source Heat Pumps (ASHP), which make use of the ambient air temperature. The subsurface temperature remains nearly constant throughout the year, in comparison with the large fluctuations of air temperature, making it easier to store or extract the larger amounts of heat.

BTES systems are often placed partly or fully in aquifers, where groundwater flow is present. Groundwater flow can occur in fractured rocky soils, or in porous soils; this study focuses on groundwater flow in porous media, which is the most common case in the Netherlands. As shown in Figure 3, there are three main processes of heat transfer in porous media: conduction (or diffusion), dispersion, and advection (caused by groundwater flow). The latter can have a significant effect on the heat transfer process of a BTES system, as heat is carried towards or away from the borehole with the groundwater flow (Chiasson et al., 2000; Su et al., 2004). However, it is often neglected, mostly due to the difficulties in computing or measuring groundwater movement (Diao et al., 2004).

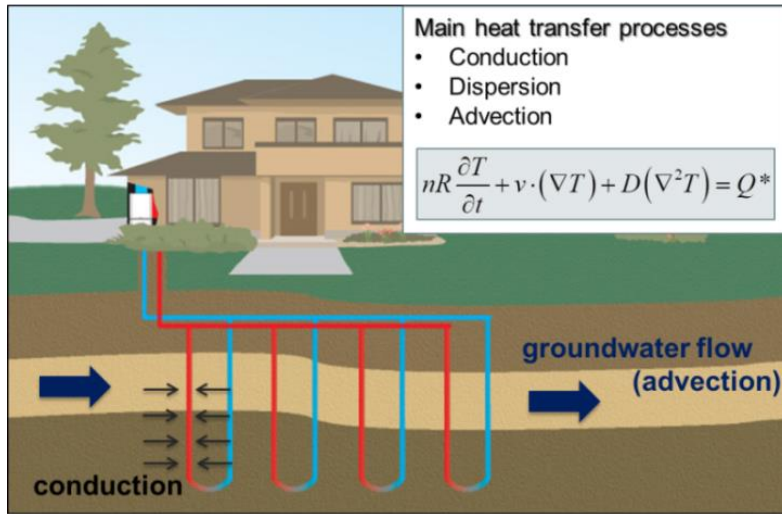


Figure 3: Main processes of heat transfer in the subsurface

## 1.2. Previous research

Research has been conducted on the influence of groundwater flow on heat transfer, using experimental or numerical approaches to assess the effect of groundwater flow on estimated thermal parameters or on resulting temperatures, but there are still large knowledge gaps in this field.

For the design of BTES systems, information is required on the ground thermal parameters (such as thermal conductivity, heat capacity and thermal resistance of the borehole). Thermal response tests (TRT), which are usually carried out to measure these parameters, often use the assumption that conduction of heat is the only heat transfer process (Bruno et al., 2013; Witte, 2012), not taking the possible presence of groundwater flow into account. This can lead to false parameter estimation; for example, in-situ measured thermal conductivities can appear higher due to advection caused by groundwater flow (Chiasson et al., 2000).

Multiple studies have shown that heat exchange rates of BTES systems are enhanced by groundwater flow (Chiasson et al., 2000; Gehlin & Hellström, 2003; Witte & van Gelder, 2006; Su et al., 2004). According to Chiasson et al. (2000), the system's performance is especially enhanced when considering heat storage, since the heat transfer is driven by temperature differences, and the advection of heat away from the boreholes allows for larger heat loads to be transferred. According to Su et al. (2004), groundwater flow can be beneficial to the performance of BTES systems in both heating and cooling modes, as it has a moderating effect on borehole temperatures.

The idea behind the ground heat exchange systems is taking advantage of the soil's temperature, which is relatively constant throughout the year, to store and extract heat. It is very common for either heating or cooling demands to be dominating in a building, resulting in imbalanced annual energy loads – for example, buildings in cold climates have a much higher demand of heating, while commercial or institutional buildings have a higher demand of cooling. In these cases, the heat exchanger lengths often need to be greater in order to compensate for this imbalance (Diao et al., 2004), or the heating and

cooling loads can be artificially balanced, for example by supplementing the excess energy need by other sources (Banks, 2012). If groundwater flow is present, and contributes in restoring the temperatures of the subsurface, then the over-designing or the necessity to include additional energy sources can be prevented by taking groundwater flow into account when designing the system (Diao et al., 2004). On the other hand, in cases where heating and cooling loads are approximately balanced, the heat buildup around the borehole is desirable, as it will enhance the forthcoming heat extraction and vice versa. Dehkordi et al. (2015) showed that for balanced systems, groundwater flow can have undesired impacts, as it appears to reduce the heat transfer rate.

Another knowledge gap concerns the effect of low groundwater flow after a long period; various studies (Angelotti et al., 2014; Dehkordi et al., 2015; Su et al., 2004) point out that it's not necessarily high flow that should be taken into account, as moderate flow can have a significant effect in the long term. Since geothermal energy storage is a relatively recent technology, no conclusions have yet been established on this subject.

Considering all the above, it is easy to conclude that groundwater flow should be taken into account in the design of BTES systems, to ensure economical sustainability and avoid over or under-design. However, this can be quite complicated. Groundwater flow is difficult to compute or measure, and an important deficiency is the lack of proper simulation tools. Only a few tools are commercially available for the simulation of BTES, and all of them are based on principles of heat conduction, completely neglecting the implications of groundwater flow (Bauer et al., 2009; Diao et al., 2004). A simulation tool is needed which will be capable of predicting the temperature profile in the underground and the performance of a BTES system under the presence of groundwater flow.

### 1.3. Scope and approach

This study aims to quantify the effect of groundwater flow on the performance of BTES systems; performance is defined as the achieved energy exchange between a system and the ground. The goal is to build a model suitable to simulate heat exchange of a BTES system under the effect of both conduction and advection, identify the main parameters that affect the system's performance, and estimate the impact of groundwater flow on the energy output of the system in both heating and cooling modes. This leads to the following research questions:

- *How is the performance of a BTES system affected by groundwater flow in case of one way heat transfer (only heating or only cooling), as well as in cases of a combined heating and cooling demand?*
- *On which parameters does this effect depend on?*

The structure of the study is as follows:

- Chapter 2: A simple case of heat transfer in the subsurface is solved analytically and numerically, in order to gain insight on the dominant processes of heat transfer, understand the analogy between the different solutions, and verify the accuracy of the numerical method applied.

- Chapter 3: A detailed 3D model is created, simulating water flowing inside a BTES system and exchanging heat with the subsurface, combined with groundwater flow. A sensitivity analysis is performed on the model, in order to assess the impact of different case-specific model parameters on the output. The model is tested using the results of an experiment, to verify its credibility.
- Chapter 4: A case study is built based on a real BTES system in the Netherlands. The system is placed in an area with low groundwater flow, which was not taken into account in the system's design. The case study simulates the heating and cooling loads of the system in the future, in scenarios with and without groundwater flow, to assess its effect.
- Chapter 5: Discussion, conclusions and recommendations.

## 2. Developing simulation method to model the effect of groundwater flow on BTES systems

In this chapter, a simple case of heat transfer in the subsurface in an area with groundwater flow is solved using three different methods: one analytical and two numerical models. The purpose of this comparison is to gain insight on the dominant processes of subsurface heat transfer and understand the analogy between the parameters of the numerical and analytical solutions. The objective is to verify the accuracy of the method used for the numerical simulation, and subsequently be able to model more complex situations based on this method.

### 2.1. Description of simulated area and assumptions

A fully saturated aquifer is assumed. There is a head difference between the west and east boundary of the area, inducing steady-state horizontal groundwater flow in the x-direction. There is a vertical line source injecting a constant rate of heat in the aquifer throughout the simulations, modeled differently in each case. The following assumptions are made:

- The thermal and hydraulic properties of the medium are homogeneous.
- The initial temperature of the aquifer is uniform, and water and solids share the same temperature.
- As the temperature changes that occur are only a few degrees, viscosity and density of water are assumed to be constant and not affected by temperature; variable –density groundwater flow does not occur.
- Heat transfer in the aquifer is driven by diffusion and advection; dispersion is neglected.

The three-dimensional heat transfer equation for these conditions can be written as (Bakker et al., 2015; Ren et al., 2000):

$$\frac{\partial T}{\partial t} = D \left( \frac{\partial^2 T}{\partial x^2} + \frac{\partial^2 T}{\partial y^2} + \frac{\partial^2 T}{\partial z^2} \right) - \frac{u}{R} \frac{\partial T}{\partial x} \quad (1)$$

Where  $T$  ( $^{\circ}\text{C}$ ) is the temperature,  $t$  (d) is time,  $D$  ( $\text{m}^2/\text{d}$ ) is the thermal diffusivity,  $R$  (-) is the thermal retardation coefficient and  $u$  ( $\text{m}/\text{d}$ ) is the constant and uniform specific discharge in the positive x direction. The specific discharge is the average fluid velocity in the pores; it is calculated as:

$$u = \frac{V}{n} \quad (2)$$

where  $V$  ( $\text{m}/\text{d}$ ) is the Darcy groundwater velocity, and  $n$  (-) is the effective porosity, which is simply referred to as porosity in this thesis. The thermal diffusivity and thermal retardation coefficient are properties of the medium defined as:

$$D = \frac{\kappa}{c\rho} \quad (3)$$

$$R = \frac{c\rho}{nc_w\rho_w} \quad (4)$$

where  $c$  (J/kg/°C) is the heat capacity and  $\rho$  (kg/m<sup>3</sup>) is the density. The retardation coefficient represents an equilibration of temperature between the fluid and solid; it causes the temperature front to move slower than the average linear flow velocity. The term  $c\cdot\rho$  (J/ °Cm<sup>3</sup>) is the volumetric heat capacity of the saturated soil, calculated as an arithmetic mean of the volumetric heat capacities of the water and the solids:

$$c\rho = n \cdot c_w \rho_w + (1-n) \cdot c_s \rho_s \quad (5)$$

The term  $\kappa$  (W/m/°C) is the bulk thermal conductivity, which can be derived from the thermal conductivities of the soil and water in different ways. It is difficult to accurately determine the bulk thermal conductivity of a porous medium, as it depends not only on the porosity but also on the shape of the grains and the pore structure.

There are three models widely used to determine the bulk thermal conductivity (Ingebritsen & Sanford, 1998): the arithmetic mean (AM), the harmonic mean (HM) and the geometric mean (GM).

$$\left\{ \begin{array}{l} (AM) : \kappa = n\kappa_w + (1-n)\kappa_s \\ (HM) : \frac{1}{\kappa} = \frac{n}{\kappa_w} + \frac{1-n}{\kappa_s} \\ (GM) : \kappa = (\kappa_w)^n (\kappa_s)^{1-n} \end{array} \right\} \quad (6)$$

The arithmetic mean and harmonic mean models form the upper and lower boundary respectively for the calculation of bulk thermal conductivity. They are both averaging the thermal conductivity based on the assumption of a layered structure of phases (in this case, layers of solids and water), where heat flows through the layers in parallel (in the arithmetic mean model), or perpendicularly (in the harmonic mean model). Both these models are independent of the pore structure (Fuchs et al., 2013). The geometric mean model is an empirical formula, which is often used as a reasonable estimation between the arithmetic and harmonic means (Johansen, 1977; Woodside & Messmer, 1961). In this thesis, the arithmetic mean was chosen for the calculation of  $\kappa$ .

A rough estimation of the effect of groundwater flow of heat transfer can be made using the defined parameters. The relative importance of advection compared to conduction in case of heat transport in groundwater flow can be quantified by the Péclet number (Anderson, 2005), which is defined as:

$$Pe = \frac{c_w \rho_w u L}{\kappa} \quad (7)$$

where  $L$  is a characteristic length. In principle, advection becomes significant when the Péclet number is of order one (Chiasson et al., 2000); of course, it is dependent on the choice of  $L$ .

The size of the simulated area is approximately 25x25 m<sup>2</sup> and the depth of the soil is 30 m. The scale of the model is relatively small – compared to the magnitudes of groundwater flow and energy input – in order to examine the heat transfer in the proximity of the heat source, while keeping the simulation time short. The specific groundwater discharge in the x-direction is  $u = 1 \text{ m/d}$  and the initial uniform temperature of the medium is  $T = 10 \text{ }^{\circ}\text{C}$ . The duration is 60 days, during which the heat injection rate is constant. The parameters used in the simulations are listed in Table 1.

**Table 1: Parameters of model**

Effective porosity	$n = 0.35$
Water density	$\rho_w = 1000 \text{ kg/m}^3$
Soil density	$\rho_s = 2650 \text{ kg/m}^3$
Bulk density	$\rho_b = (1-n)\rho_s = 1722.5 \text{ kg/m}^3$
Heat capacity of water	$c_w = 4100 \text{ J/kg/K}$
Heat capacity of solids	$c_s = 850 \text{ J/kg/K}$
Volumetric heat capacity of soil	$\rho c = n\rho_w c_w + (1-n)\rho_s c_s = 2.9 \text{ MJ/m}^3/\text{K}$
Thermal conductivity of water	$\kappa_w = 0.58 \text{ W/m/K}$
Thermal conductivity of solids	$\kappa_s = 2.8 \text{ W/m/K}$
Thermal conductivity of soil	$\kappa = n\kappa_w + (1-n)\kappa_s = 2 \text{ W/m/K}$
Thermal diffusivity	$D = \kappa/\rho c = 0.06 \text{ m}^2/\text{d}$
Thermal retardation coefficient	$R = cp/nc_w\rho_w = 2.0$

In the next paragraphs, the setup of each model is explained and the model results are compared and analyzed.

## 2.2. Description of the models

### 2.2.1. Analytical “line-source” model

According to Chiasson et al. (2000), one of the most common analytical models for heat transfer in the subsurface is the “line-source” (Ingersoll et al., 1955; Kelvin et al., 1882); a borehole heat exchanger of sufficient length with respect to its radius can be considered as a line source, and this approach is widely used for systems of this type (Witte, 2012). Here, it is applied as explained in Bakker et al. (2015). The heating source is modeled as an infinitely long line source vertical to the plane of flow – in this two-dimensional version of the analytical solution, the line source is a point source, and the heat injection rate is per meter depth. The source is heated at a constant and uniform rate  $q$  (W/m), starting at time  $t = t^*$ . The temperature increase as a function of time and space can be written as:

$$\Delta T(x, y, t, t^*) = \frac{q}{4\pi\kappa} \exp\left(\frac{u \cdot x}{2DR}\right) \int_{\frac{x^2+y^2}{4D(t-t^*)}}^{\infty} \frac{1}{s} \exp\left(-s - \frac{1}{s} \frac{u^2(x^2+y^2)}{16D^2R^2}\right) ds \quad (8)$$

where  $\Delta T$  ( $^{\circ}\text{C}$ ) is the temperature difference caused by the heating source, and  $x$  and  $y$  (m) are the coordinates of points with reference to the point where the heating source is placed.

### 2.2.2. Numerical “cable” model (2D)

In this model, groundwater flow and heat transfer are modeled in a 2D horizontal plane with one thick uniform soil layer; changes in the vertical direction are neglected. The model simulates a heating cable inserted vertically in the soil. The cable is in direct contact with the aquifer material and injects a specified amount of heat.

The tools used for the simulation are MODFLOW (Harbaugh, 2005) and MT3D (Bedekar et al., 2016). MODFLOW is a finite-difference model for groundwater flow, and MT3D is a model for multispecies solute transport in porous media. Temperature is modeled as a solute in MT3D, since the governing equations for solute transport are mathematically identical to those for heat transfer (Hecht-Méndez et al., 2010). The methodology of the heat transfer simulation with MT3D is applied according to Langevin et al. (2008). The input and output of the model is processed via the open source Python package FloPy (Bakker et al., 2016).

The assumption was made that viscosity and density of water are constant with temperature, and therefore that the flow is not affected by temperature changes. This was confirmed by initially using SEAWAT (Langevin et al., 2008), a coupled version of MODFLOW and MT3D that simulates variable-density groundwater flow, to carry out the simulation. The outcome of the SEAWAT model was compared to the outcome of a model where MODFLOW and MT3D were performing the simulations separately: MODFLOW simulates the flow, and MT3D uses the output of MODFLOW to simulate heat transfer. From the results it was clear that there was no effect of variable-density flow. The flow is independent from the heat transfer and the two don't have to be modeled in parallel – SEAWAT was therefore not used.

The model is two dimensional – a single 30m thick layer is used to simulate the aquifer. The horizontal 25x25 m<sup>2</sup> plane is modeled with varying cell sizes: dense gridding of 3.5x3.5 cm is used close to the heating source, increasing to 2x2 m near the boundaries. This is done in order to achieve higher accuracy of the simulation in the center of the field where the effect of temperature increase is most pronounced, while simultaneously keeping the runtime and required memory low. As the direction of groundwater flow is parallel to the X-axis, the heat source is placed on the X-axis, and all the properties of the aquifer are uniform, the model is symmetrical with respect to the X-axis; therefore only half of the area is modeled, further decreasing the runtime and memory by half.

#### ➤ Flow solution: MODFLOW

##### Properties and boundary conditions

The type of aquifer is confined and fully saturated. The east and west boundaries of the model consist of constant head cells with a head difference, inducing groundwater flow from the west to the east. The north and south boundaries of the model are defined as no-flow boundaries. Steady state conditions are applied throughout the flow simulation. The hydraulic conductivity  $K_H$  is 7 m/d.

## Solver

The flow model is solved with the Preconditioned Conjugate Gradient (PCG) method. The PCG solver uses two levels of iteration (outer and inner iterations) and two criteria for convergence.

- Head change criterion: for every iteration, the solver compares the head in each cell with the head calculated in the previous iteration. The criterion is met when the maximum absolute value of head change between two iterations is smaller than  $10^{-5}$ .
- Residual criterion: for every iteration, the solver compares the difference between inflows and outflows for each cell. The criterion is met when the absolute value of the difference is smaller than  $10^{-5}$ .

Both criteria must be met for convergence to be achieved.

The model grid, boundaries and flow solution of MODFLOW are presented in Figure 4.

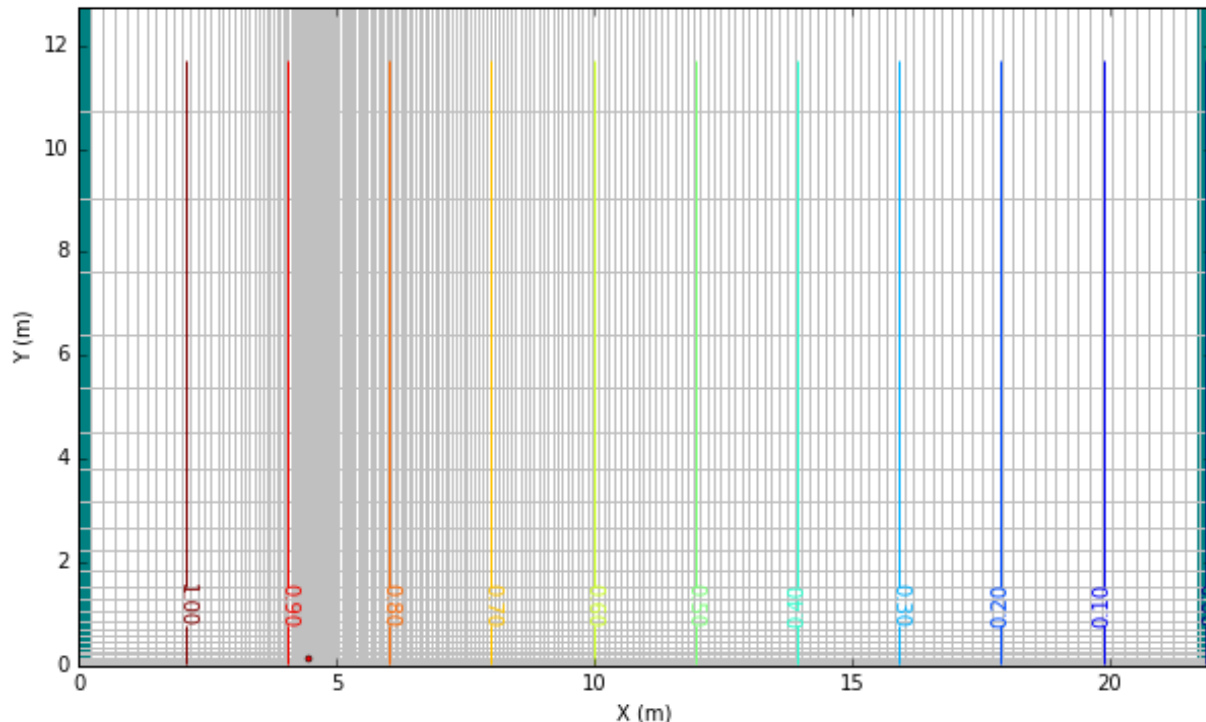


Figure 4: Top view of grid, boundaries and heads of the 2D numerical “cable” model. The east and west boundaries consist of constant head cells. The red dot in the part with denser grid spacing indicates the position of the heat source. The contours indicate hydraulic head.

## ➤ *Heat transfer: MT3D*

### Properties and boundary conditions

MT3D uses the flow solution of MODFLOW to simulate solute or heat transfer. The configuration of the area is the same as for MODFLOW. The north and south boundaries are defined as zero heat flux boundaries. The east and west boundaries, which consist of constant head cells in MODFLOW, are specified heat flux cells in MT3D; the specified amount of heat entering and exiting the domain is determined by the inflow and outflow of water, which has been calculated by MODFLOW.

### Analogy to the analytical solution

The general form of the solute transport equation used by MT3D is (Thorne et al., 2006):

$$\left(1 + \frac{\rho_b K}{n}\right) \frac{\partial(nC)}{\partial t} = \nabla \left[ n \left( D_m + \alpha \frac{v}{n} \right) \nabla C \right] - \nabla(vC) - q_{src} C_{src} \quad (9)$$

where  $C$  ( $\text{kg}/\text{m}^3$ ) is the solute concentration,  $\rho_b$  ( $\text{kg}/\text{m}^3$ ) is the bulk density,  $n$  (-) is the porosity,  $\alpha$  ( $\text{m}$ ) is the dispersivity tensor,  $v$  ( $\text{m}/\text{d}$ ) is the Darcy groundwater velocity,  $q_{src}$  ( $\text{d}^{-1}$ ) is the source or sink of fluid and  $C_{src}$  ( $\text{kg}/\text{m}^3$ ) is the concentration of the solute at the source.

The general heat transfer equation can be written in the following form, to point out the analogy with (9):

$$\left(1 + \frac{1-n}{n} \frac{\rho_s c_s}{\rho_w c_w}\right) \frac{\partial(nT)}{\partial T} = \nabla \left[ n \left( \frac{\kappa}{n \rho_w c_w} + \alpha \frac{v}{n} \right) \nabla T \right] - \nabla(vT) - q_{src} T_{src} \quad (10)$$

Where  $T$  ( $^\circ\text{C}$ ) is the temperature, and all the parameters have been defined in Table 1. The left hand side of the equation is the rate of temperature increase, multiplied by the retardation coefficient (equation 3). On the right hand side, the first term represents diffusion and dispersion of heat, the second term is the advection of heat caused by groundwater flow, and the last term stands for the source of heat.

By taking the assumptions made here into account, and replacing thermal diffusivity  $D$  (3) and retardation  $R$  (4) into (10), it becomes:

$$\begin{aligned} R \cdot n \cdot \frac{\partial T}{\partial t} &= D \cdot R \cdot n \cdot (\nabla^2 T) - v \cdot (\nabla T) - q_{src} T_{src} \Rightarrow \\ \frac{\partial T}{\partial t} &= D \cdot (\nabla^2 T) - \frac{u}{R} \cdot (\nabla T) - Q_{src} T_{src} \end{aligned} \quad (11)$$

Where  $u = v/n$  ( $\text{m}^3/\text{d}$ ) is the specific groundwater discharge, and  $Q_{src} = q_{src}/nR$ . Expressed in this form, is clear that (11) is the same as the two-dimensional version of the heat transfer equation (1), including a source term.

### Retardation

The retardation coefficient  $R$  defined in (4) can be expressed as:

$$R = 1 + \frac{1-n}{n} \cdot \frac{c_s \rho_s}{c_w \rho_w} = 1 + \frac{1-n}{n} \cdot \rho_s \cdot K_d \quad (12)$$

Where  $K_d$  ( $\text{m}^3/\text{kg}$ ) is the thermal distribution coefficient, defined (for saturated soil) as:

$$K_d = \frac{c_s}{c_w \rho_w} \quad (13)$$

The retardation of heat transfer is mathematically similar to linear sorption in solute transport. The reaction package (RCT) is used in MT3D to model retardation as linear sorption. Parameters  $K_d$ ,  $n$ , and  $\rho_b$  are defined in this package.

### Thermal diffusivity

As it can be seen when comparing (9) and (10), the molecular diffusion coefficient  $D_m$  for solute transfer corresponds to the following term in the heat transfer equation:

$$D_{m\_temp} = \frac{\kappa}{n \rho_w c_w} = \frac{n \kappa_w + (1-n) \kappa_s}{n \rho_w c_w} \quad (14)$$

The term  $D_{m\_temp}$  ( $m^2/day$ ) is referred to as bulk thermal diffusivity and is introduced to the model through the dispersion package (DSP).

### Advection

Advection is simulated in MT3D using the ADV package. The standard FD method is chosen instead of the third-order TVD scheme. The TVD scheme is considered to have higher accuracy, as it minimizes numerical dispersion (Zheng & Wang, 1999); however, it consumes much more memory and significantly increases running time. In this case, choosing the standard FD method in the advection package decreased the running time by a factor of  $10^3$  in the 3D model (2 seconds instead of 80 minutes), while the results were similar for both methods. This test served as a verification of the accuracy of the FD method, in order to safely implement it in the more complex models that followed, as it would be unfeasible to apply the TVD scheme in models with longer time scales.

### Sinks and sources

The last term of (10) is a volumetric sink/source of pre-defined temperature. All sources and sinks of water and/or heat can be included in MT3D through the sink and source mixing package (SSM), where a temperature and a type of source needs to be defined. In this model, as heat is added to the system through a heating cable, the “mass-energy loading” type is used. The appropriate “solute-equivalent” amount of energy to enter the SSM package is a variable denoted as  $M_T$  ( $^{\circ}\text{C}\cdot\text{m}^3/\text{day}$ ). In analogy with the analytic solution,  $M_T$  is defined as (Langevin et al., 2008):

$$M_T = \frac{E}{\rho_w c_w} \quad (15)$$

where  $E$  (J/day) is the amount of energy per unit time, calculated from the heat flux  $q$  (W/m) of (8) as:

$$E = q \cdot L \cdot (3600 \cdot 24) \quad (16)$$

where  $L$  is the length of the heat exchanger.

The energy added to the system is entered in one cell and averaged over that cell.

#### Solver

The GCG solver, an iterative solver based on the Generalized Conjugate Gradient method, is used in the simulation. When the standard FD method has been selected in the advection package, as in this case, GCG solves all the terms of the governing equation (advection, sink/source and reaction terms) implicitly, without any stability constraints (Zheng & Wang, 1999). It has two iteration loops (inner and outer loop) and its convergence criterion is met when the absolute difference of relative concentration (in this case, temperature) between two successive iterations is smaller than  $10^{-5}$  for all cells.

#### **2.2.3. Numerical “pipe” model (3D)**

Contrary to the cable model, the pipe model is three-dimensional. It simulates water flowing through a pipe, similar to the pipes used in BTES systems, inserted vertically in the soil. Water enters the pipe at the surface and exits at the bottom layer; the temperature of the water entering the pipe ( $20^{\circ}\text{C}$ ) is higher than the ambient temperature of the soil ( $10^{\circ}\text{C}$ ), and thus heat is absorbed by the soil. The 30 m thick soil is modeled as fifteen layers of 2 m.

The pipe model is simulated using MODFLOW and MT3D. The configuration of the system, packages and parameters applied are generally the same as in the cable model, with a few differences that will be explained in this section.

##### **➤ Flow solution: MODFLOW**

In the same way as in the cable model, the aquifer is confined and fully saturated, and constant head cells are used in the east and west boundaries to induce horizontal groundwater flow. The north and south sides, as well as the top and bottom layers are defined by MODFLOW as no-flow boundaries. The main difference in this case is the way that the heat source is modeled. The cable model simulates an energy input that is added to the system through a heating cable; this process is independent from the flow simulation and is only included in the heat transfer simulation. On the other hand, the pipe model simulates warm water flowing through a pipe and transmitting heat to the soil; the volumetric flow inside the pipe needs to be simulated with MODFLOW. This is done as follows:

The top of the pipe is simulated as a well (using the WEL package), which injects a constant flow of water in the system. The size of the cell where the well is placed is 3.5x3.5 cm and the inflow is 22.5  $\text{m}^3/\text{day}$ , producing a velocity of approximately 0.2 m/s in the pipe. The bottom of the pipe is simulated as a constant hydraulic head cell. To make sure that water flows straight through the pipe from the top to the bottom (without any interaction with the surrounding groundwater), all the cells that compose the pipe have specific hydraulic properties: the horizontal hydraulic conductivity ( $K_H$ ) is set to zero, the vertical hydraulic conductivity ( $K_V$ ) is set to a very large number (500 m/d) and the porosity ( $n$ ) is set to 1. In all the other cells, the normal hydraulic parameters of the aquifer are applied, as defined in the cable model. With this setup, the volume of water injected in the top layer can only flow downwards to

the next layers until it reaches the constant head cell in the bottom – no water can flow to the adjacent cells in the horizontal direction.

The schematization and the properties of the 3D pipe model are pictured in Figure 5.

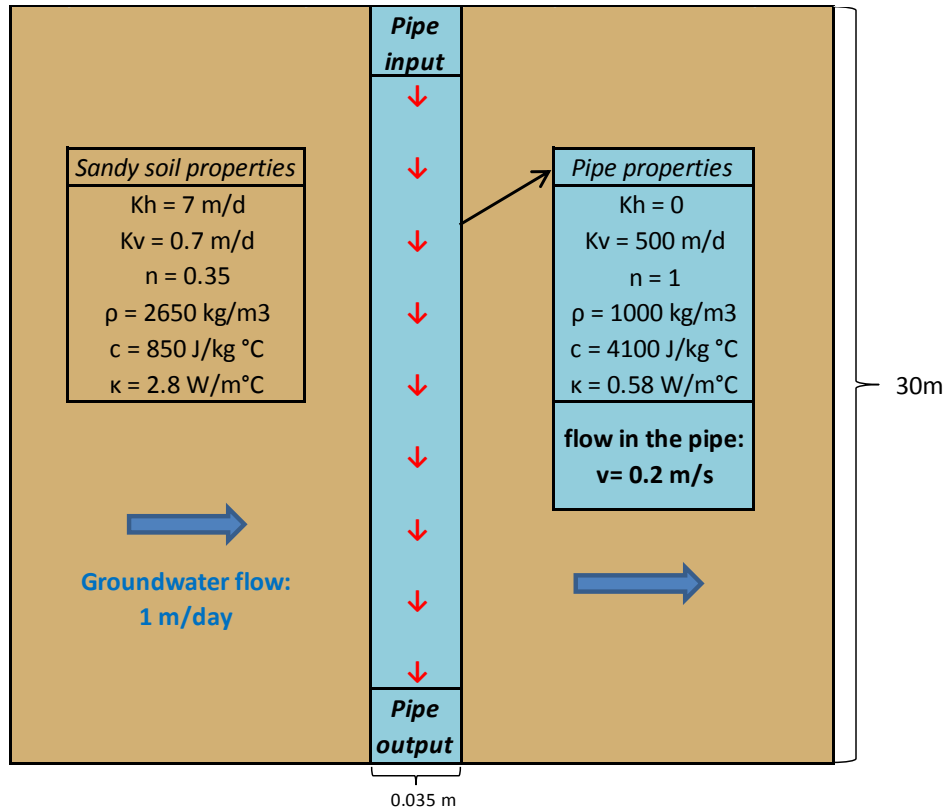


Figure 5: Schematization of a cross-section of the 3D numerical “pipe” model

### ➤ Heat transfer: MT3D

#### Thermal parameters

Parameters  $K_d$ ,  $n$ ,  $\rho_b$  and  $D_m$  are defined through the reaction, advection and dispersion packages, as explained in the cable model. For the cells that are part of the pipe, different values are used, as those cells are simulated to contain only water and no soil. The difference in the parameters is pictured in the schematization of Figure 5. The heat source is modeled differently from the cable model. In this case, where a volume of warm water is injected at the source, the “well” type is chosen in the SSM package. The input temperature of the water injection ( $20^\circ\text{C}$ ) is also defined for this type.

#### Analogy with the line-source and cable models

As water flows through the pipe, energy in the form of heat is absorbed by the soil. This amount of energy can be calculated based on the flow rate in the pipe and the temperature difference between the two ends of the pipe. For the cable model, the  $M_T$  variable used in the SSM package is computed based on the output of the pipe model:

$$M_T = \Delta T_{\text{pipe}} \cdot Q_{\text{flow}} = (T_{\text{in}} - T_{\text{out}}) \cdot Q_{\text{flow}} \quad (17)$$

where  $Q_{\text{flow}}$  ( $\text{m}^3/\text{day}$ ) is the flow rate in the pipe,  $T_{\text{in}}$  ( $^{\circ}\text{C}$ ) is the given input temperature at the top of the pipe,  $T_{\text{out}}$  ( $^{\circ}\text{C}$ ) is the output temperature at the bottom of the pipe. Consequently, for the line-source model, the heat injection rate  $q$  ( $\text{W}/\text{m}$ ) is calculated using (15) and (16).

## 2.3. Results

The resulting distribution of heat in the soil around the source is compared for all three models and can be seen in Figures 6 - 9. For the most part, the numerical models follow the analytical solution, with discrepancies appearing at the point of the source (where the exact temperature cannot be accurately calculated), as well as some small fluctuations between 10 and 20 from the source in the X direction. These fluctuations are most probably caused by instability of the numerical integration of the analytical line source model, and are not indicators of actual inconsistencies of the results.

As the absolute differences are lower than  $0.2^{\circ}\text{C}$  (Figure 8) and the errors are lower than 10% (Figure 9), it can be safely concluded that the results are realistic and the method is suitable for simulation of heat transfer.

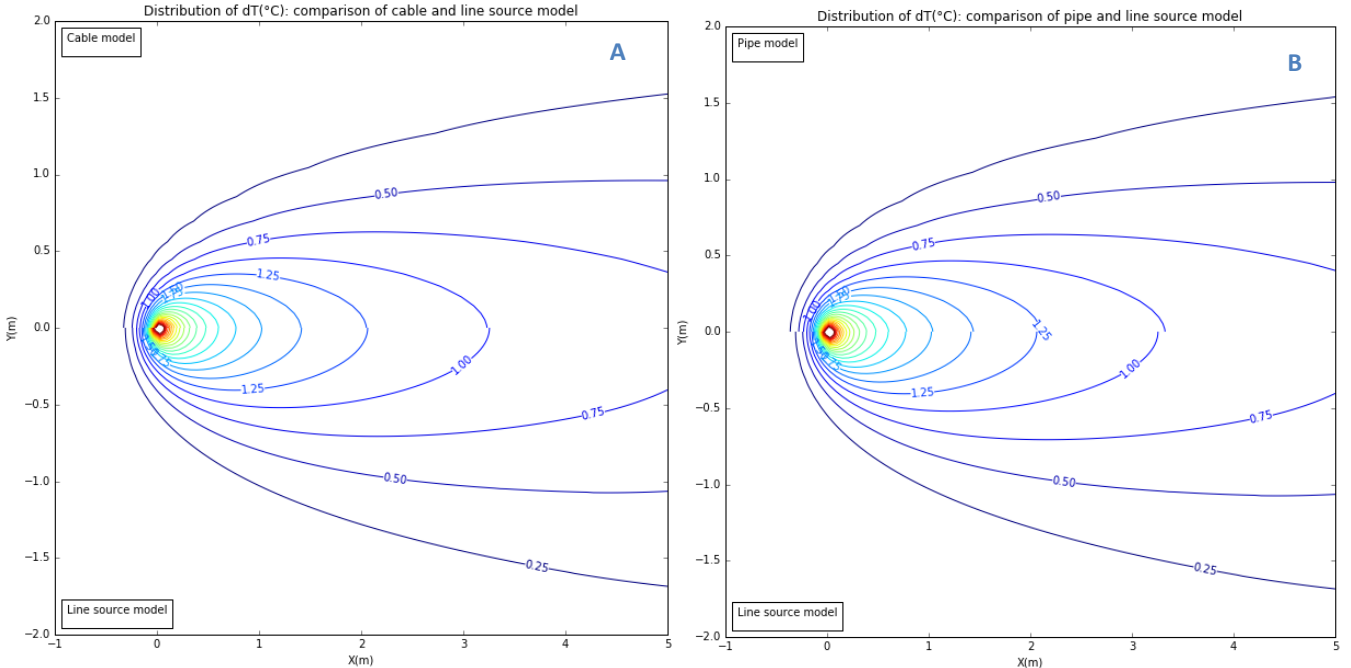


**Figure 6: Distribution of the temperature increase in the soil around the heat source at the end of the 60 day period.**

**A:** Comparison of the cable model (top half) and line source model (bottom half).

**B:** Comparison of the pipe model (top half) and the line source model (bottom half). For the pipe model, the middle soil layer is plotted.

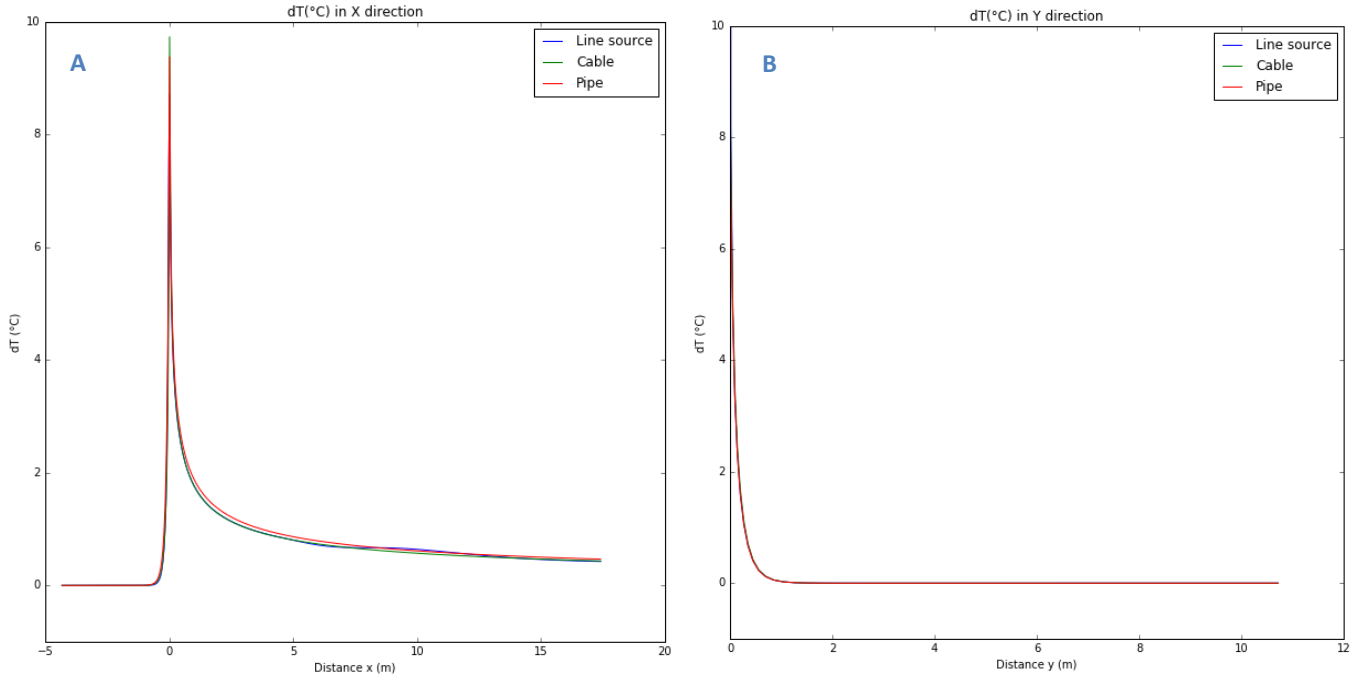


**Figure 7: Distribution of temperature increase in the soil along cross sections crossing the heat source. Comparison between the 3 models at the end of the 60 day period. For the pipe model, the middle soil layer is plotted.**

**A: Cross section in the X direction**

**B: Cross section in the Y direction**

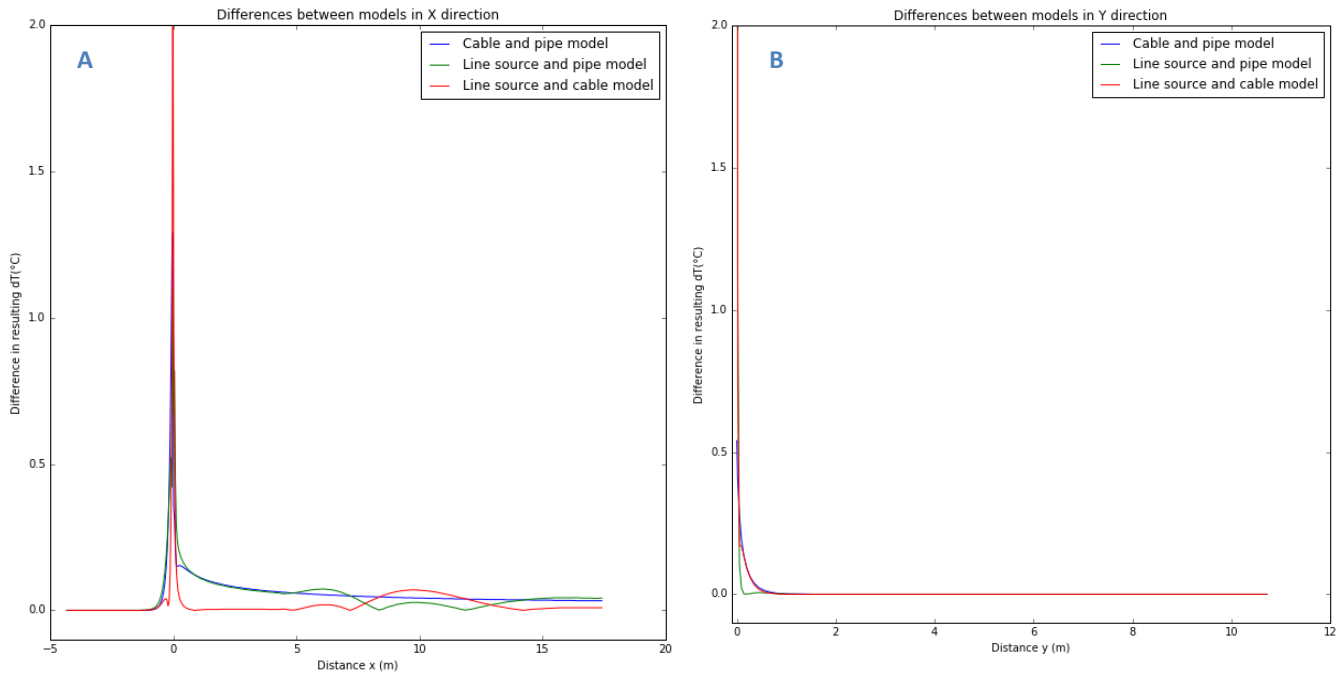


**Figure 8: Differences between the distributions of temperature increase of Figure 7.**

**A: Cross section in the X direction**

**B: Cross section in the Y direction**

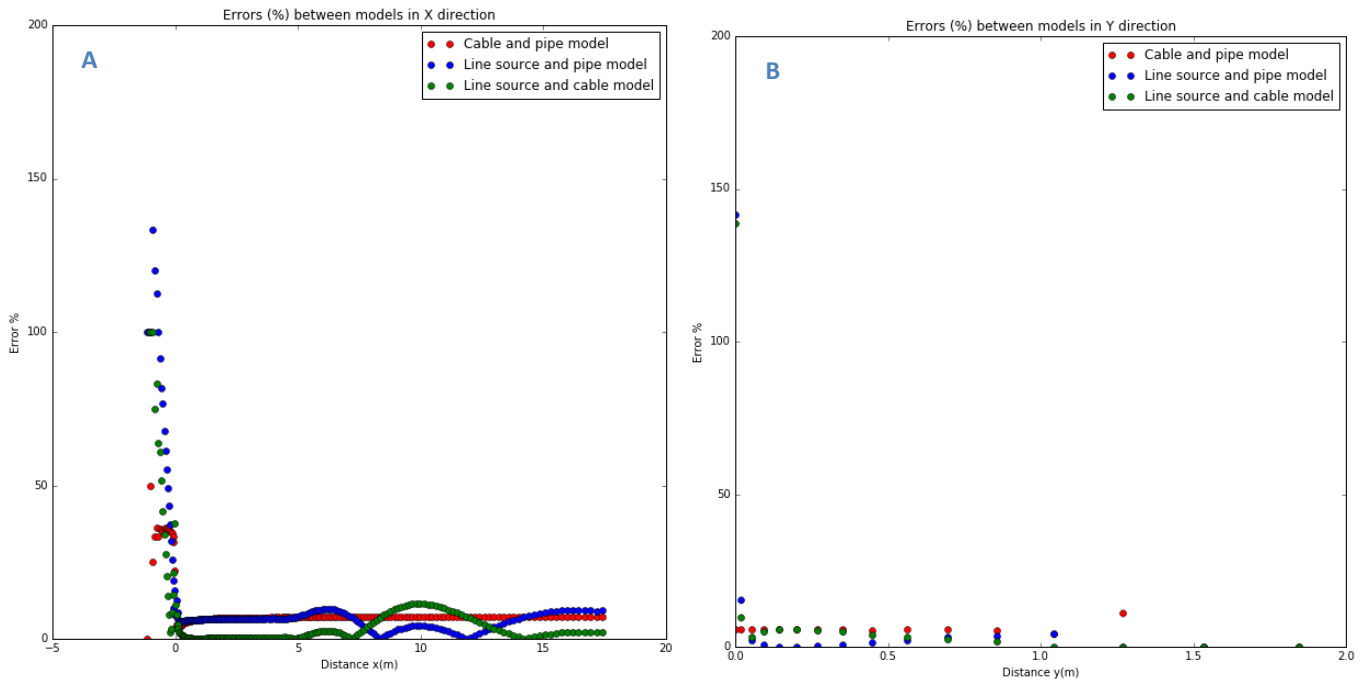


**Figure 9: Relative errors (%) between the distributions of temperature increase of Figure 7.**

**A: Cross section in the X direction**

**B: Cross sections in the Y direction**

### 3. Main BTES model

After the results of the 3D numerical model of the straight pipe have been verified, the main model is constructed based on the same methodology. This is a model of a vertical loop that will be used to simulate a case study of a typical BTES system. A sensitivity analysis is performed to assess the effect of different model parameters on the output.

#### 3.1. Description

The schematization and main properties of this model are displayed in Figure 10 and Figure 11. Regarding the parameters of the aquifer and the pipe, realistic values that can be found in BTES systems in the Netherlands are applied. The model simulates a U-shaped pipe that is inserted vertically into the soil in a 150 m deep borehole – the total length of the pipe is therefore 300 m. The size of the area is approximately 60x70 m<sup>2</sup>, which is discretized with cells of varying sizes, increasing with distance from the borehole. The two parts of the pipe are close together, at a distance of 3.5 cm. As the model is symmetrical with respect to the X axis, only half of the area is simulated, and the resulting plots are reflected on the X-axis to illustrate the whole area.

The north and south boundary, as well as the top and bottom layer, are defined as no-flow boundaries in MODFLOW and no-heat-flux boundaries in MT3D. The east and west boundaries are simulated as constant head cells in MODFLOW, and specified heat flux cells in MT3D, where the specified amount of heat entering and exiting the domain is determined by the inflow and outflow of water calculated by MODFLOW.

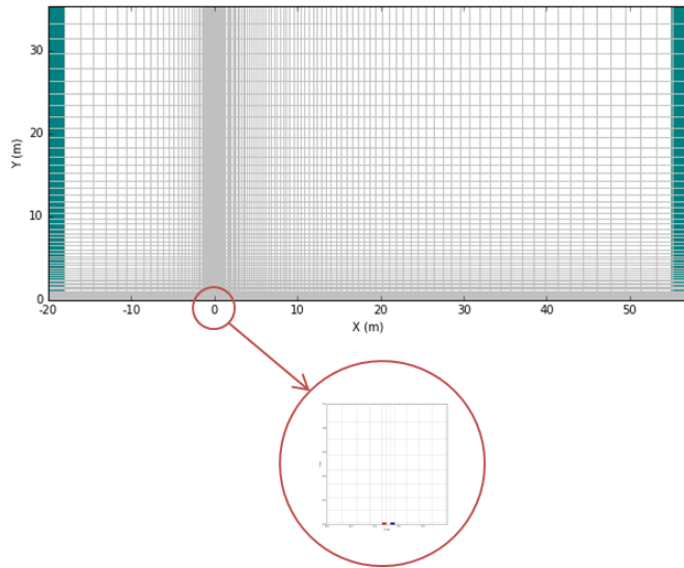


Figure 10: Horizontal cross-section of grid and boundaries of the main 3D BTES model (top layer). The east and west boundary are constant head cells; the circled point at the thicker part of the grid indicates the position of the borehole. The two colored cells are the input (red) and output (blue) of the BTES pipe. Note: The size of the domain was enlarged for some of the simulations, by extending the west boundary to -60 m and placing the BTES system in the middle of the X-axis.

All the boundaries are placed far enough from the BTES system to not affect the calculations of heat distribution in the soil; in some of the simulations, the west boundary had to be moved further away

from the borehole to prevent its interference with the resulting heat distribution (e.g. in the sensitivity analysis, paragraph 3.4.3 - A). As for the top and bottom layer, they are placed right above and below the borehole; their interference with heat transfer is considered insignificant, as the diameter of the borehole is very small compared to its length and heat transfer in the vertical direction is negligible compared to the horizontal direction.

The hydraulic and thermal properties of the soil are the same as in the previous section, but the specific groundwater discharge has been reduced to 0.025 m/day. That is a commonly occurring value for aquifers in the Netherlands, where flow rates are slow – only a few meters per year (Pellenbarg, 1997). The ambient temperature of the soil is 10 °C and a well injects water of 20 °C at the input point of the pipe, at a rate such that the flow velocity in the pipe will be 1 m/s. In the descending and ascending parts of the pipe, the cells are designed as denoted in Figure 11; the porosity ( $n$ ) of 1, the large value of hydraulic conductivity in the vertical direction ( $K_v$ ) and the null value in the horizontal direction ( $K_h$ ) ensure that the water flow follows the defined route. The turning point at the bottom is trickier;  $K_h$  cannot be zero at this point, as water has to flow horizontally towards the ascending pipe. Instead, inactive cells (no-flow boundaries) are placed around the pipe at the bottom layers to prevent leakage.

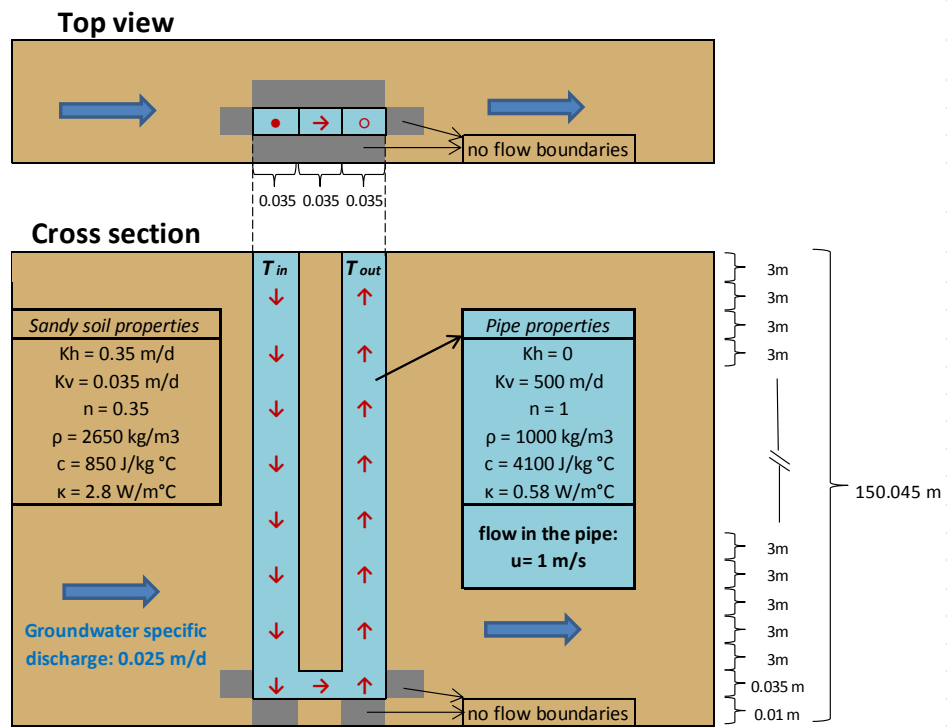


Figure 11: Schematization (top view and cross section) of the BTES system and its properties as simulated in the 3D model.

The model simulates a 25-year long period of continuous heat storage (so a BTES system operating only for cooling). This large time scale was required for the temperature distribution in the soil to reach a steady state, due to the low level of groundwater flow. The BTES system is assumed to be constantly on for the whole duration of the simulation.

The resulting distribution of temperature in the pipe and in the soil is presented in the results.

### 3.2. Results

As it can be seen from the shape of the temperature distribution in Figure 12 (compared with the case of no groundwater flow) and Figure 13, the influence of groundwater flow is not easily noticed in the short term, but becomes more and more pronounced in the long term. This is rational, since the assumed value of groundwater flow is quite low (2.5 cm/day or 9 m/year); it takes a few years before the changes in temperature distribution become obvious. The effect of groundwater flow is more pronounced in large distances from the borehole. This can also be derived from the Pécelt number (7), which is in the order of one for a characteristic length L larger than 2 m, meaning that heat transfer is advection-dominated at distances longer than 2 m from the borehole.

The results show that at this level of groundwater flow, the distribution of heat in the soil becomes stable approximately after 18.8 years (90% stabilization, meaning that after 18.8 years, the temperatures at all points have reached 90% of the value they have at the end of the 25-year period). Groundwater flow contributes to reaching a steady-state situation of heat exchange, as it drives down the rising temperatures around the borehole by carrying heat away. In the case where there is no groundwater flow, the temperatures near the borehole keep increasing and in consequence, the heat transfer from the BTES to the soil keeps decreasing. This is further analyzed in the sensitivity analysis (3.4.3-A).

The temperature difference between the input and output points of the pipe is 0.532 °C, a value that is stabilized after the first 5 years of the simulation time. The temperature distribution along the two parts of the pipe in different time steps is presented in the graph of Figure 14. In spite of the seemingly symmetrical distribution of temperature along the two parts of the pipe, the temperature at the bottom of the pipe (turning point) is lower than the average of the input and output temperatures, which means that more heat is transmitted to the ground from the descending part of the pipe than the ascending part. This is because the temperature gradient between the BTES and the ground, which drives the heat exchange, becomes lower as the circulating water loses heat.

The temperature difference is reasonable, although lower than expected, as in reality the gain or loss of temperature in BTES systems is approximately 3-4 °C. There are multiple reasons for this discrepancy, as the model makes use of some simplifying assumptions. For example, the filling material of the borehole (which can enhance the conduction of heat) is not included in the simulation, and neither is conductivity of the pipe walls. Also, the model does not account for inhomogeneity in the thermal properties and the background temperature of the ground; in reality, the temperature of the subsurface is not entirely uniform with depth, and especially in the top soil layers there are temperature variations throughout the year. Another important difference is that the model simulates continuous heat injection with a fixed input temperature, while a real system would be turned off or switched to heat extraction for some time. An intermittent heat injection would allow the soil around the BTES to cool down, and subsequently absorb more heat, while a continuous heat injection leads to a heat buildup around the BTES that reduces the heat exchange capacity.

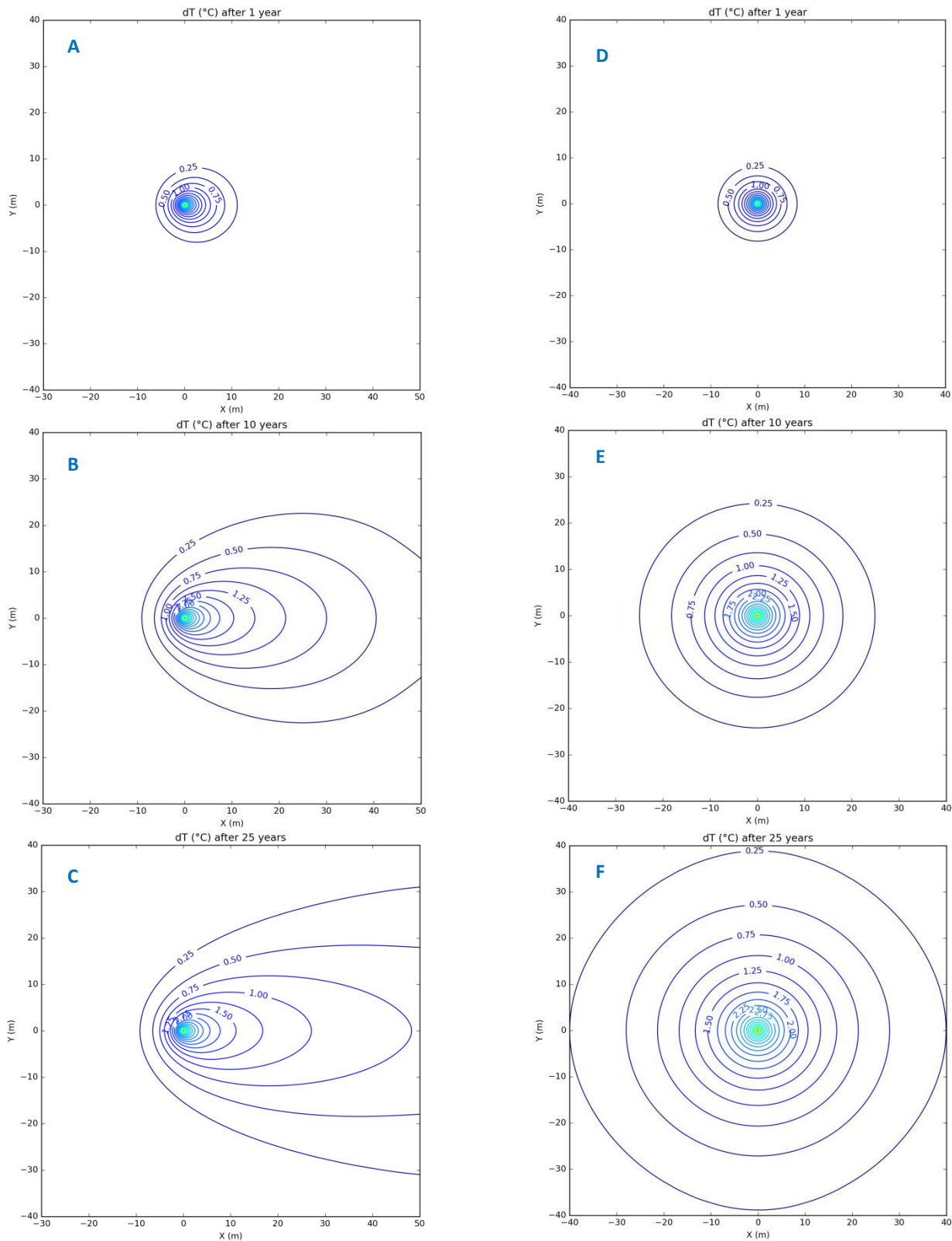


**Figure 12: Distribution of temperature increase at different time steps in the soil layer around the bottom of the borehole.**  
**Figures A, B and C show the distribution with the presence of constant groundwater flow; Figures D, E and F show the distribution at the same time steps when there is no groundwater flow.**

The equivalent rate of energy transfer from the BTES to the soil for this temperature difference is calculated as:

$$E = M_T \cdot \rho_w c_w = \Delta T \cdot Q_{flow} \cdot \rho_w c_w = 0.532 \cdot 105.84 \cdot 4.1 = 230 \text{ MJ/day}$$

which is reasonable, compared to energy extraction data provided by Itho-Daalderop (that fluctuate in a wide range between 150 and 300 MJ/day). This is an indication that the assumed flow rate of the pipe might be higher than in real systems – since the temperature drop  $\Delta T$  is lower than expected, but the energy rate is in the right order of magnitude. This will be further explored in the sensitivity analysis (3.4.3-B).

Figure 15 depicts the cumulative rate of energy transfer from the BTES system to the soil, along the length of the pipe. From the gradually decreasing slope of the curve it is clear that the rate is not constant, as it might appear from the temperature distribution in the pipe in Figure 14; the rate is decreasing at each point along the length of the pipe, as the circulating water gradually loses heat and the temperature gradient between the soil and the BTES decreases.

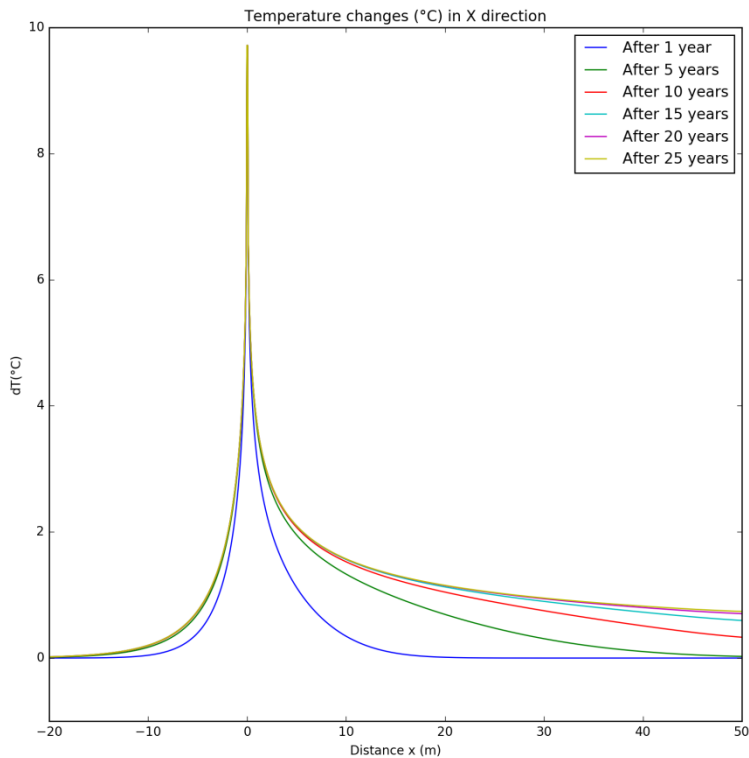


**Figure 13: Distribution of temperature increase in the soil along a cross section crossing the bottom of the BTES system, in the direction of the flow, for different time steps.**

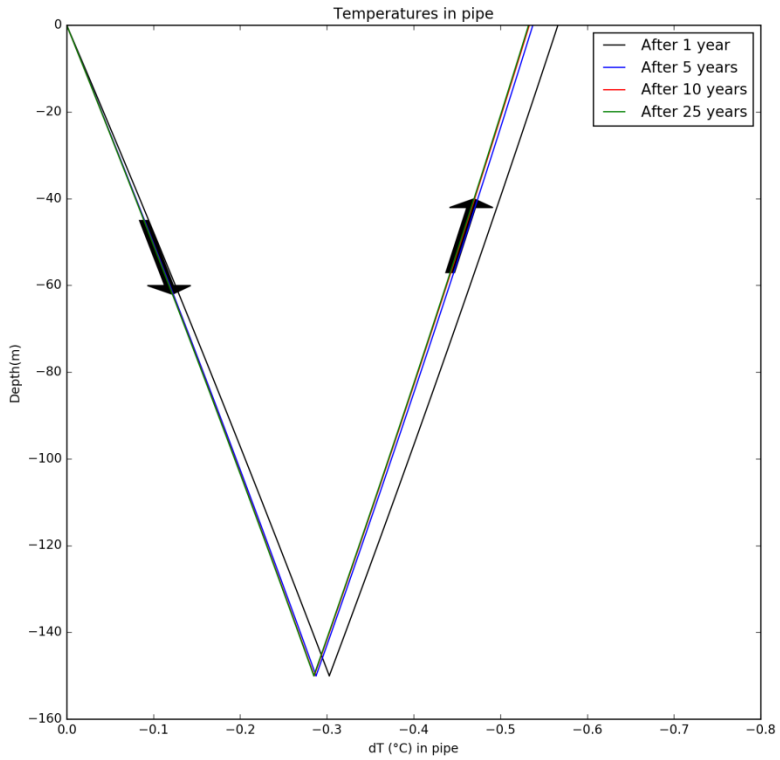


**Figure 14: Distribution of temperature decrease in the pipe, for different time steps. Arrows indicate the direction of flow.**

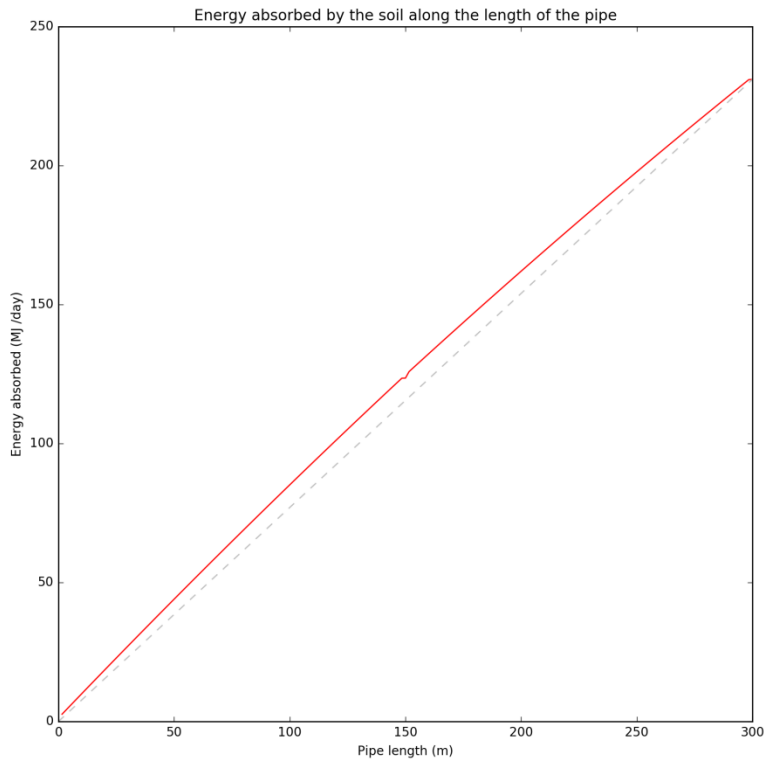


**Figure 15: Cumulative energy flux rate absorbed by the soil for each point along the pipe (after the heat exchange rate has been stabilized). The dashed line indicates a hypothetical linear distribution of energy flux rate, for reference purposes.**

### 3.3. Verification of model

The developed model is used to simulate two geothermal response tests conducted by Groenholland (Witte & van Gelder, 2006), in order to test its accuracy. The tests were performed on Groenholland's reference BTES system. Each test comprised three energy pulses: two heat injection pulses at different energy levels and one heat extraction pulse, with a recovery period between injection and extraction. During the first test, there was no groundwater flow, while during the second test an extraction well located 2.5 m away from the BTES induced groundwater flow.

The two experiments are simulated with the 3D BTES model using the measured or estimated parameters listed in Table 2. The recorded temperatures, flow rates in the BTES pipe, and well extraction rates are provided by Groenholland. The duration of each experiment is 4 days, which is simulated as 96 stress periods of 1 hour.

The aquifer is confined and fully saturated. The borehole filling is included in the simulation. The soil and the borehole filling are both sandy materials, but have different characteristics. The circulating fluid is a 17% glycol mixture. The background soil temperature during the experiment was 15°C, which is assumed to be uniform in the simulation. The 30 m of depth are simulated with thirty 1 m thick layers. An area of 30 x 30 m<sup>2</sup> is simulated using a grid of varying cell sizes. The round pipe is modeled with a square cell of equal surface. The BTES system and extraction well are placed on the X-axis; the area is symmetrical with reference to the X-axis and the half-grid approach is applied.

**Table 2: Model parameters used to simulate Groenholland's geothermal response test. For parameters marked with \***  
assumptions were used, followed by some calibration.

	<b>Soil (sandy)</b>	<b>Borehole filling material</b>	<b>Circulating fluid (glycol)</b>
Thermal conductivity $\kappa$	2.2 W/m °C	1.8W/m °C	0.35W/m °C
Volumetric heat capacity $\rho \cdot c$	2500 J/m <sup>3</sup> °C	2250 J/m <sup>3</sup> °C	3974 J/m <sup>3</sup> °C
Porosity n *	0.4	0.2	-
Hydraulic conductivity $K_H$ *	10 m/d	-	-
Soil temperature	15 °C	Pipe diameter	25 mm
Borehole depth	30 m	Pipe flow rate	0.7 m <sup>3</sup> /h
Borehole diameter	0.25 m	Well extraction rate	40 m <sup>3</sup> /d

The plots of Figure 16 compare the measured average temperatures of the circulating fluid in the BTES systems with the temperatures calculated from the model, for the two experiments. The model follows the pattern of the experimental results, although there is some underestimation of the temperature during the second heat injection pulse and the heat extraction pulse by approximately 0.2 °C. Of course, the model is based on some simplifying assumptions and cannot simulate the full complexity of an experiment; for example, hydraulic conductivity and porosity are based on estimations, and the model does not take the parameter of borehole resistance into account (which can have an effect on the heat exchange between the two parts of the U-pipe), or the fact that soil temperature might not be uniform.

However, as the relative errors between the modeled and measured temperatures of the fluid are lower than 10% in any time step, it is safe to conclude that the model offers a realistic approximation of the temperatures of a BTES system in both heating and cooling.

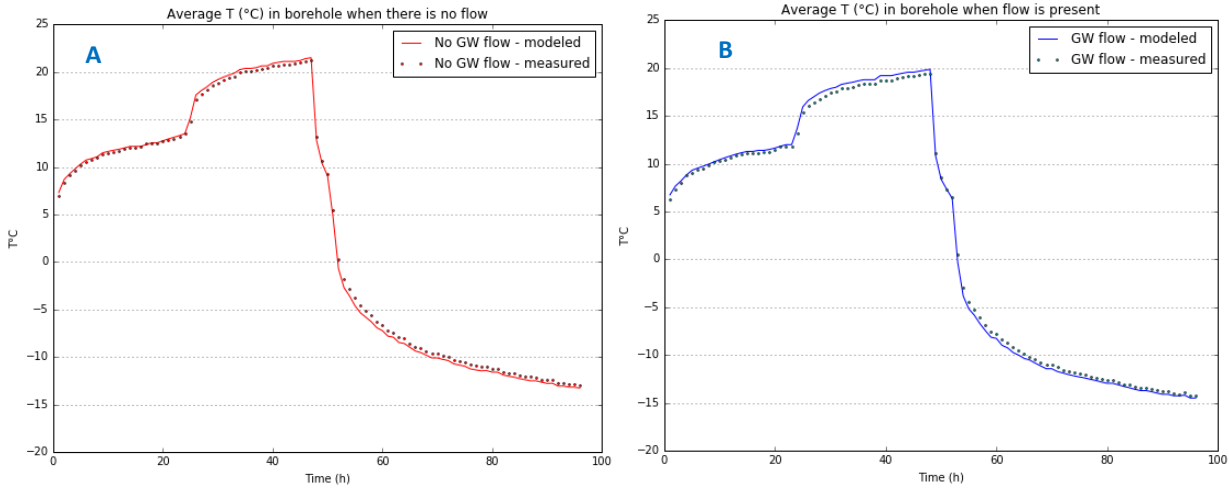


Figure 16: Average temperatures of fluid in BTES system. Comparison of modeled and measured temperatures for the reference experiment (A) and the experiment with groundwater flow (B).

### 3.4. Sensitivity analysis

A sensitivity analysis was performed on the BTES model, in order to assess the impact of each parameter on the system output. The simple one-at-a-time method was used: multiple scenarios were tested, with one parameter being altered in each scenario while the others kept their initial value.

#### 3.4.1. Scenarios

In Table 3, an overview of the parameters and scenarios of the sensitivity analysis is presented. Various parameters are chosen for different reasons. Some of them (such as the velocity of the circulating water and the number of systems) are depending on the system and can be controlled. The purpose is to quantify their effect on the system output, in order to figure out how they can be adjusted to achieve a better performance (heat exchange capacity) of the system. Other parameters (such as the groundwater flow or the soil porosity) depend on the system's environment and cannot be controlled, but the sensitivity analysis aims to provide more insight into their positive or negative effect, so that the system can be accordingly calibrated.

Scenario 0 is the reference case – as presented in 3.1 – to which each of the other scenarios is compared.

Scenarios A1 and A2 test the effect of a 50% decrease or increase of the groundwater discharge respectively, while scenario A0 tests the case where there is no groundwater flow. As the main scope of this study is to assess the effect of groundwater flow on the performance of BTES systems, this analysis serves as a quantification of this effect by comparing different magnitudes of groundwater flow, which make the heat transfer process less or more conduction-dominated, as well as the case of no groundwater flow, which makes the heat transfer purely conductive.

Scenarios B1 and B2 test the effect of a 50% decrease or increase respectively on the velocity of the water circulating in the pipe. The volume of water flowing through the system in a given amount of time is expected to have a strong effect on the output temperatures, but it is more important to see if there is an effect on the resulting energy exchange.

Scenarios C1 and C2 test the effect of lower and higher soil porosity compared to the reference case. The porosity is a parameter that can influence heat exchange in different ways, as the ratio of water and solids determines the lumped thermal parameters of the soil – density, heat capacity and thermal conductivity (equations (3) – (6)) – as well as the specific groundwater discharge. Changes in porosity therefore have an effect on both the conduction and advection components of the heat transfer equation (1), and the sensitivity analysis aims to investigate the overall effect on the system's outcome.

Scenarios D1 and D2 test the effect of higher or lower background soil temperatures. The initial temperature of the soil forms the temperature gradient that drives the heat exchange; it is therefore directly related to the output temperatures of the system.

Scenario E tests a change in the configuration of the input and output of the pipes. In the reference case, the two parts of the pipe were placed in parallel with the direction of groundwater flow, with the output pipe downstream. In scenario E they are reversed by 180°, as shown in Figure 17. There are other possible combinations for the configuration (e.g. 90°), but only the 180° shift scenario is tested, as it is expected to have the maximum difference in output in comparison with the reference case.

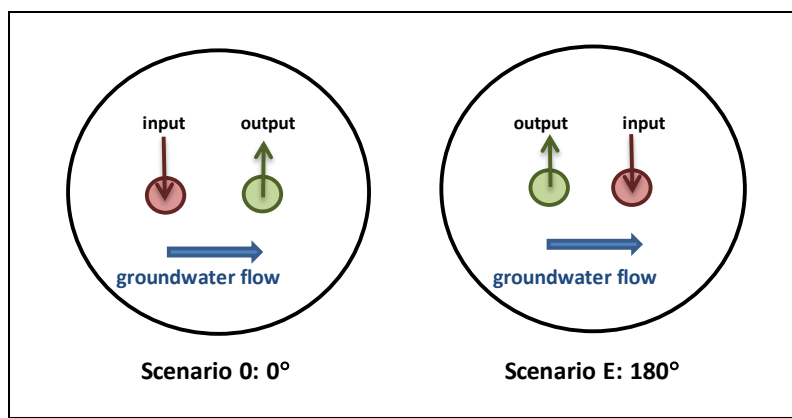


Figure 17: Configuration of pipes in scenarios 0 and E

In scenarios F1 – F4, cases of groundwater flow occurring in different parts of the aquifer along the borehole length are examined. In real systems, it is more common for groundwater flow to occur at certain depths, as in a vertical cross section of the subsurface there are usually alternations of different types of soils, as well as permeable and impermeable layers. This analysis looks into the effect of groundwater flow, depending on the points of the borehole length at which it occurs.

In scenario G, the case of a second BTES system placed downstream of the original one is tested. This case aims to look into the combined effect of groundwater flow and mutual interaction between BTES systems.

**Table 3: Parameters and scenarios of sensitivity analysis**

SENSITIVITY ANALYSIS							
Parameters	Initial values (Scenario 0)	Scenarios					
<b>Groundwater discharge</b>	0.025 m/d	<b>A1</b>	0.0125 m/d	<b>A2</b>	0.0375 m/d	<b>A0</b>	0
<b>Pipe flow velocity</b>	1 m/s	<b>B1</b>	0.5 m/s	<b>B2</b>	1.5 m/s		
<b>Soil porosity</b>	0.35	<b>C1</b>	0.28	<b>C2</b>	0.42		
<b>Background soil temperature</b>	10°C	<b>D1</b>	5°C	<b>D2</b>	15°C		
<b>Pipe configuration</b>	0°	<b>E</b>	180°				
<b>Soil layers with flow</b>	Whole aquifer	<b>F1</b>	Top 50%	<b>F2</b>	Bottom 50%		
		<b>F3</b>	Top 30%	<b>F4</b>	Bottom 60%		
<b>Number of BTES systems</b>	Single BTES	<b>G</b>	Two BTES				

### 3.4.2. Output parameters

For each scenario, the outcome of the model is compared with the initial model (scenario 0). The parameters compared in the results are:

- The temperature difference  $\Delta T$  (°C) between the input and output of the pipe, at the end of the 25 year period. The temperature difference is an indicator of the system's performance, as it is directly related to the energy transfer rate.
- The energy transfer rate  $E$  (MJ/day) achieved by the system. This is calculated from the resulting  $\Delta T$  and the flow rate in the pipe as:

$$E = (T_{in} - T_{out}) \cdot Q_{flow} \cdot \rho_w c_w$$

- The time that it takes for the temperature distribution in the soil to reach 90% stabilization (considering the temperatures at the end of the 25 year period to be stabilized). Since the reference model needs a long time before reaching steady-state, the sensitivity analysis looks into the parameters that can accelerate or slow down this process.
- The temperatures in the soil at selected points downstream of the borehole, at the end of the 25 year period; this is an indication of how far can heat be transferred in each case. The three selected points are at approximately 10, 30 and 50m downstream.

The results and conclusions for each scenario are presented in the next sections.

### 3.4.3. Results

#### A. Groundwater discharge

In the main scenario, groundwater flows with a specific discharge of 0.025 m/d (which corresponds to a Darcy velocity of  $8.75 \cdot 10^{-3}$  m/d). The specific discharge is decreased by 50% in scenario A1 and raised by 50% in scenario A2, while in scenario A0 it is set to zero. The effect of each scenario on the output parameters is summarized in Table 4. This set of scenarios was simulated for a 25-year period as well as a 100-year period, to point out the changes in temperature distribution.

**Table 4: Sensitivity analysis results for scenarios A1, A2 and A0: Different groundwater discharge. The listed numbers correspond to the end of the 100 year long simulation**

Scenarios	A0	A1	0	A2
<b>Groundwater discharge (m/day)</b>	<b>0</b>	<b>0.0125</b>	<b>0.0250</b>	<b>0.0375</b>
dT downstream (°C)	10m	2.487	1.900	1.550
	30m	1.432	1.180	0.960
	50m	1.135	0.943	0.758
Stabilization time (years)	-	38	18.8	12.2
dT output (°C)	0.403	0.486	0.532	0.564
Energy flux (MJ /day)	174.88	210.90	230.86	244.74

The changes in groundwater flow have an apparent effect on the downstream temperature distribution and an even more pronounced effect on the temperatures in the pipe, as it can be seen in Figure 18 and 19. For faster groundwater flow, the water at the pipe output comes out colder; larger amounts of heat are carried away from the borehole, allowing the system to dispose more heat to the soil. This is a positive effect for a BTES system, as the energy exchange is enhanced.

The downstream temperatures of the soil after it has reached steady state become slightly lower with higher groundwater flow. This is reasonable, as the heat travels further away; the “heat bubble” expands and temperature gradients become smoother.

The time it takes for the soil temperature distribution to reach steady state is highly dependent on the level of groundwater flow. In scenario A2, where groundwater flow is increased by 50%, stabilization time is reduced by approximately 35% compared to the reference case. On the other hand, in scenario A1, the temperature distribution is still unstable by the end of the 25-year simulation, as it takes longer to reach steady state. This can be seen in Figure 18-A; the downstream temperatures of scenario A1 should be higher compared to A2 and 0, but at long distances (>30m) they have not been stabilized yet. Graph B of Figure 18-B illustrates the temperature distribution after 100 years, when the temperature distribution has reached steady state for scenarios 0, A1 and A2.

For scenario A0, where there is no groundwater flow, the system does not reach steady state. As long as there is a continuous heat injection, the temperature near the borehole is constantly rising; the temperature gradient between BTES and soil is decreasing, and so is the heat exchange. For this reason, the results cannot be directly compared with the results of the other scenarios; again, it can be seen in Figure 18-A that downstream temperatures in scenario A0 are higher than the other scenarios in proximity of the borehole, and lower at larger distances. In the 100 year long simulation, the temperatures of scenario A0 keep rising and exceed the temperatures of the other scenarios, as is shown in Figure 18-B.

The effect here is very clear: strong groundwater flow alleviates the temperatures around the borehole, allowing the system to reach steady-state faster, and to achieve higher heat exchange.

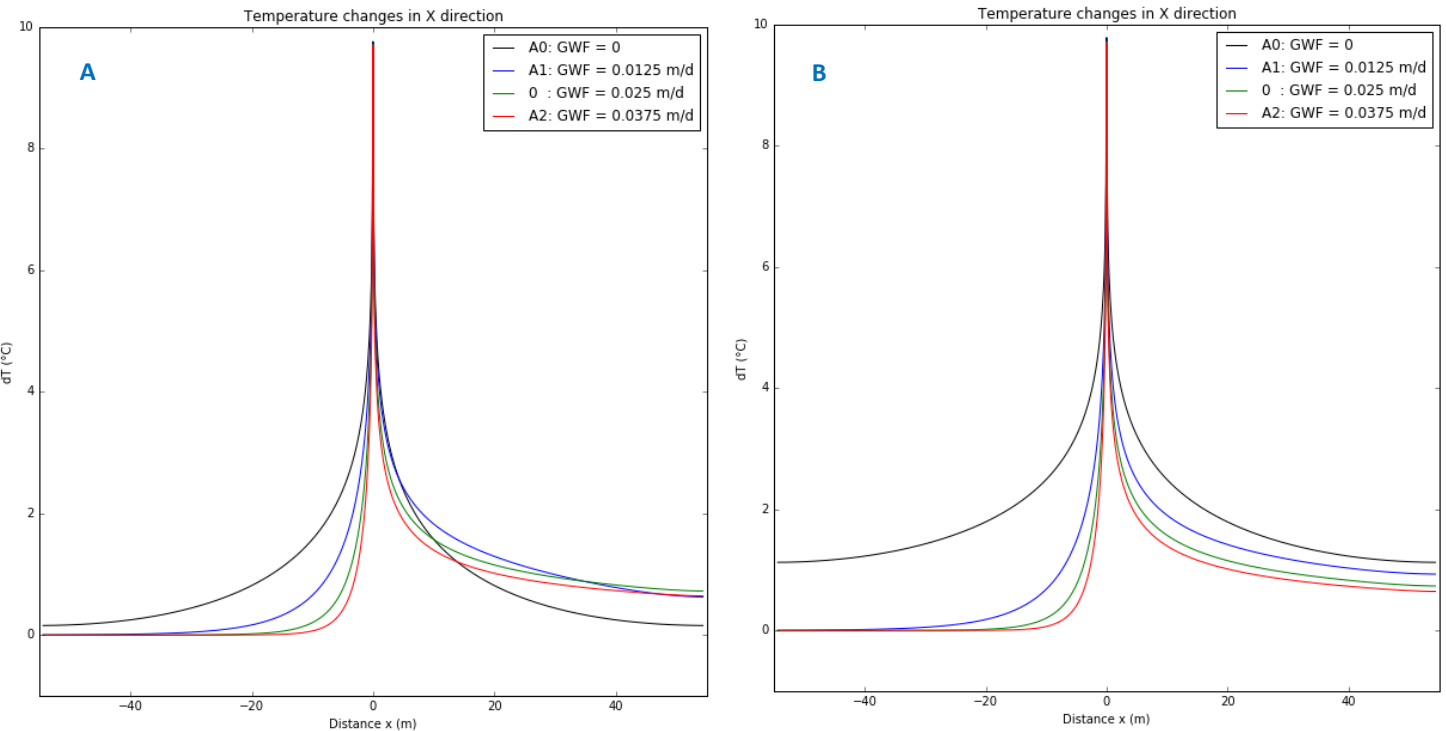


**Figure 18: Comparison of the distribution of soil temperature increase for different levels of groundwater discharge (GWF).**  
The cross section is crossing the bottom of the BTES system in the direction of groundwater flow.

A: After 25 years. B: After 100 years.

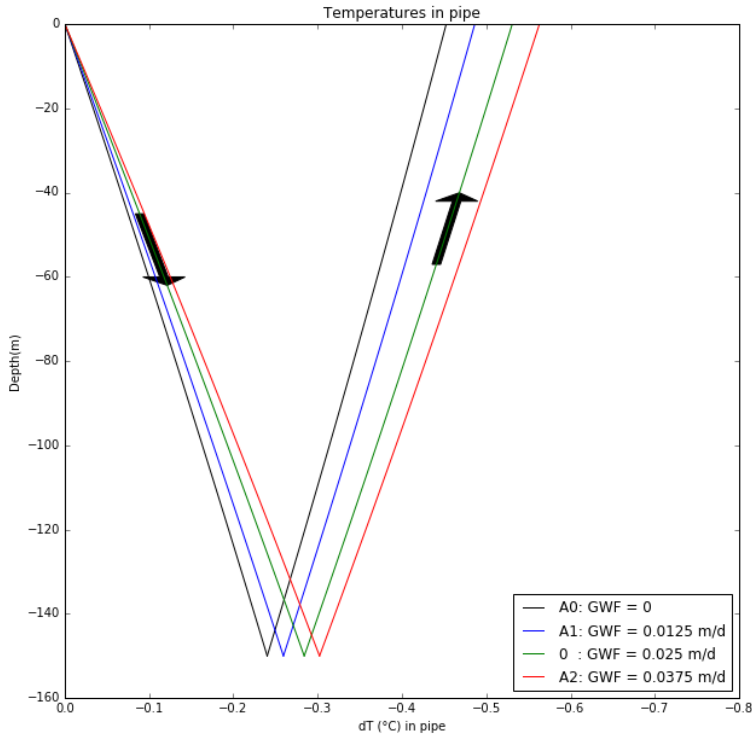


**Figure 19: Comparison of the distribution of temperature decrease in the pipe for different levels of groundwater discharge (GWF). Arrows indicate the direction of flow in the pipe.**

### B. Pipe flow velocity

The velocity of the water circulating in the pipe is 1 m/s in the main scenario, a value that is in accordance with the order of magnitude of real BTES systems. It is reduced to 0.5 m/s in scenario B1 and increased to 1.5 m/s in scenario B2. The overview of the outcome is presented in Table 5.

Changes in the circulating velocity have a negligible effect in the soil temperature distribution and no effect on the stabilization time, but the effect on the output temperature of the system is very high. This is reasonable, as lower velocities allow more time for heat exchange to take place, although it doesn't mean that the system becomes more efficient by lowering the velocity. The total energy exchanged between the system and the soil is a function of the temperature exchange and the volume of water flowing per time unit. So, by looking at Table 5, it becomes clear that in fact, higher velocities result in higher energy exchange. But again, this doesn't mean that the system efficiency will be maximized by maximizing the velocity, as the energy consumption of the circulation pump would also increase. To determine the velocity for which the total efficiency is maximized, the relationship between the velocity and the energy exchange has to be compared with the system's pump curve, in order to find the (case-specific) optimal level.

**Table 5: Sensitivity analysis results for scenarios B1 and B2– Different pipe flow velocity**

Scenarios	B1	0	B2	
Pipe flow velocity (m/s)	0.5	1	1.5	
dT downstream ( $^{\circ}\text{C}$ )	10m	1.501	1.55	1.565
	30m	0.931	0.96	0.97
	50m	0.735	0.758	0.766
Stabilization time (years)		18.8	18.8	18.8
dT output ( $^{\circ}\text{C}$ )		1.033	0.532	0.358
Energy flux (MJ /day)	224.13	230.86	233.03	

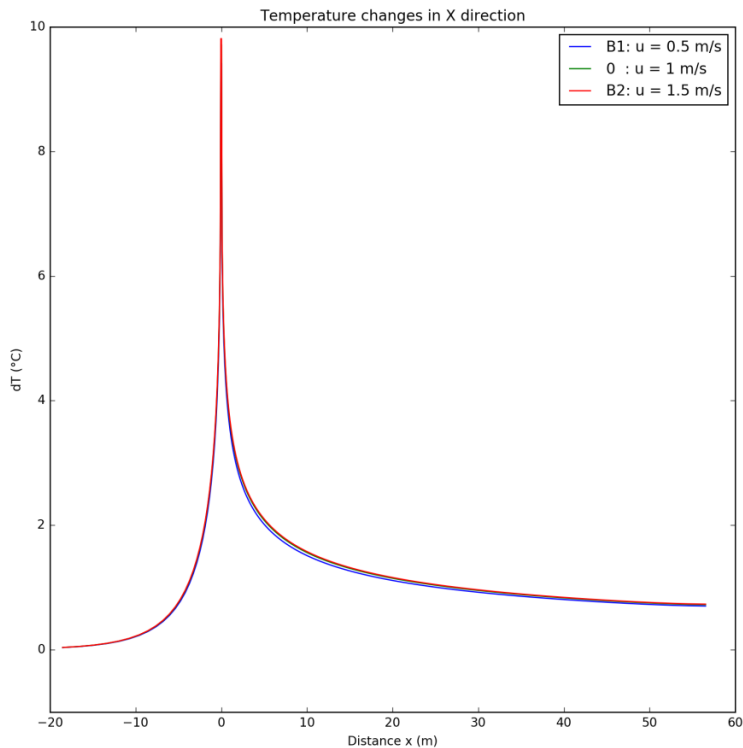


**Figure 20: Comparison of the distribution of soil temperature increase for different levels of pipe flow velocity (u). The cross section is crossing the bottom of the BTES system in the direction of groundwater flow.**

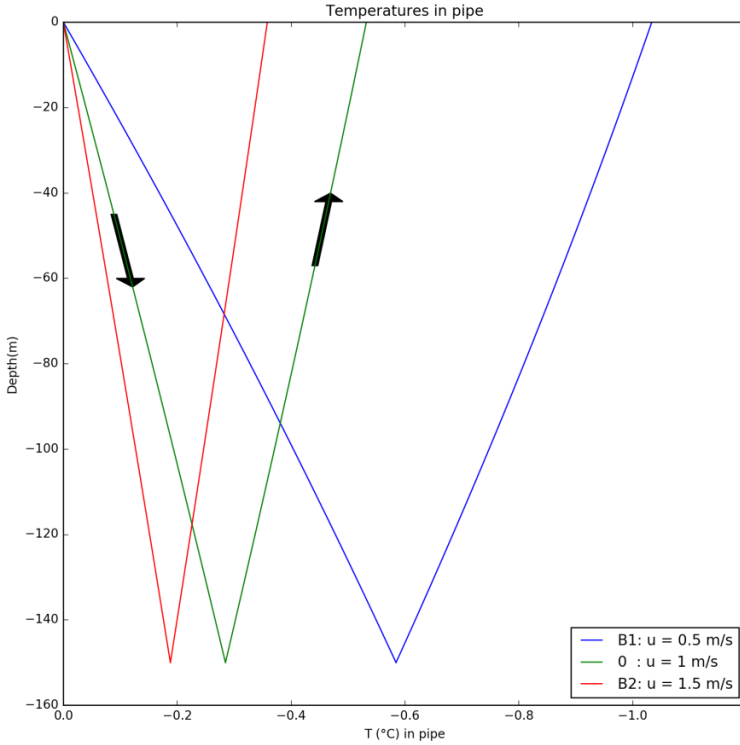


**Figure 21: Comparison of the distribution of temperature decrease in the pipe for different levels of pipe flow velocity (u).  
Arrows indicate the direction of flow in the pipe.**

### C. Soil porosity

The uniform soil porosity in scenario 0 is assumed to be 0.35, an average value for sandy soils. The range of values for porosity that can be found in coarse sands is between 0.26 and 0.43 ([geotechdata.info](#)). In both of the sensitivity analysis scenarios, the tested values of porosity are close to the minimum and maximum of this range: In scenario C1 porosity is lowered to 0.28 (20% reduction from scenario 0), and in scenario C2 it is raised to 0.42 (20% increase from scenario 0). An overview of the results is presented in Table 6.

From the results it looks like even for these high variations of the porosity, the distribution of heat in the soil is not significantly affected, even in the vicinity of the borehole. This is because the change in soil porosity affects diffusion and advection in opposite ways. This is easily noticed when looking at the heat transfer equation (1). An increase in soil porosity leads to a decrease of the molecular diffusion coefficient  $D$ , but also a decrease of the term  $u/R$ ; so when groundwater flow is present, the two effects compensate for each other, and as a result the overall effect of porosity on the temperature distribution becomes insignificant.

When looking at the temperatures in the pipe, though, the effect is clear: lower porosity does amplify the heat exchange. Also, the system reaches steady-state temperature distribution slightly faster for lower porosity, as the specific groundwater discharge (2) becomes larger.

**Table 6: Sensitivity analysis results for scenarios C1 and C2: Different soil porosity**

Scenarios	C1	0	C2
Soil porosity (-)	0.28	0.35	0.42
dT downstream ( $^{\circ}\text{C}$ )	10m	1.629	1.55
	30m	1.016	0.96
	50m	0.81	0.758
Stabilization time (years)		18.2	18.8
dT output ( $^{\circ}\text{C}$ )		0.583	0.532
Energy flux (MJ /day)	252.99	230.86	211.76

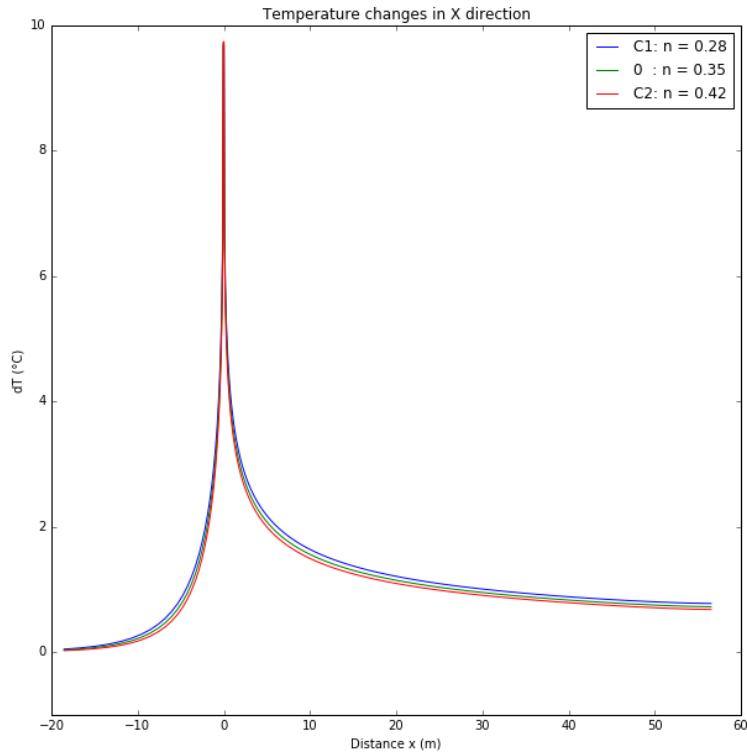


**Figure 22: Comparison of the distribution of soil temperature increase for different values of porosity (n). The cross section is crossing the bottom of the BTES system in the direction of groundwater flow.**

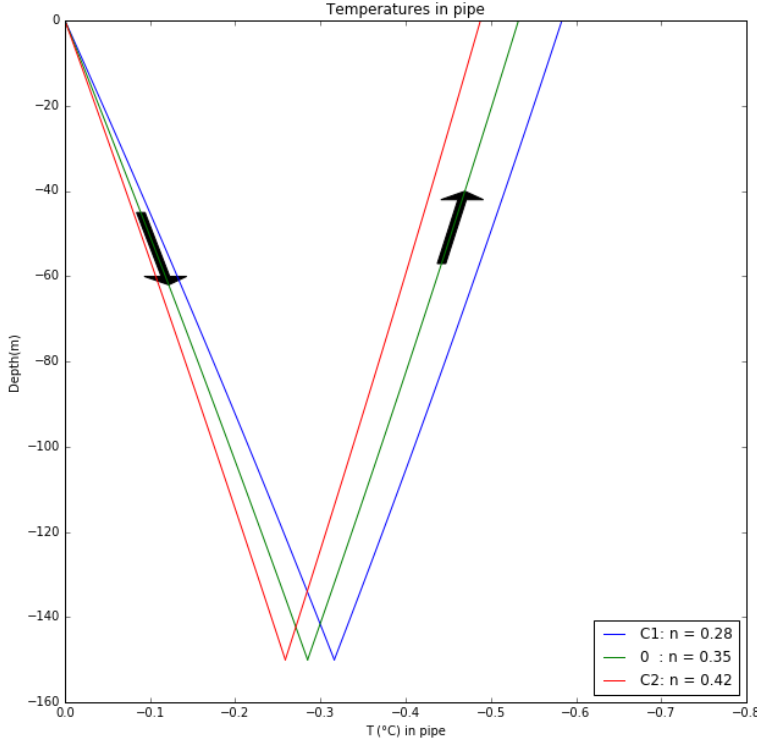


**Figure 23: Comparison of the distribution of temperature decrease in the pipe for different values of porosity (n). Arrows indicate the direction of flow in the pipe.**

#### D. Background soil temperature

In scenario 0, a uniform background temperature (i.e. the initial temperature of the soil at the beginning of the simulation) of 10 °C is assumed for the soil, which is lowered to 5 °C in scenario C1 and raised to 15 °C in scenario C2. The results are summarized in Table 7.

As expected, these high changes in background temperature have a strong effect on the temperature gradient between the circulating water and the soil, resulting in very pronounced effects both in the temperature exchange of the BTES system and in the soil temperature distribution. The effects are clear from the graphs of Figure 24 and 25.

An interesting observation in this case is that the soil temperature and the output temperature difference of the BTES system seem to be directly proportionate. More values of soil temperature within the range 5-20 °C were tested in the model to verify this, and the results are plotted in Figure 26. It becomes clear that the relationship between the output temperature and the initial soil temperature is exactly linear. This is explained by the heat transfer equation (1), as the temperature change of a specific point at a given time is directly proportionate to the temperature gradients that develop around it.

**Table 7: Sensitivity analysis results for scenarios D1 and D2: Different background soil temperature**

Scenarios	D1	0	D2
Background soil temperature (°C)	5	10	15
dT downstream (°C)	10m	2.325	1.55
	30m	1.443	0.96
	50m	1.144	0.758
Stabilization time (years)		18.6	18.8
dT output (°C)		0.799	0.532
Energy flux (MJ /day)		346.72	230.86
			115.43

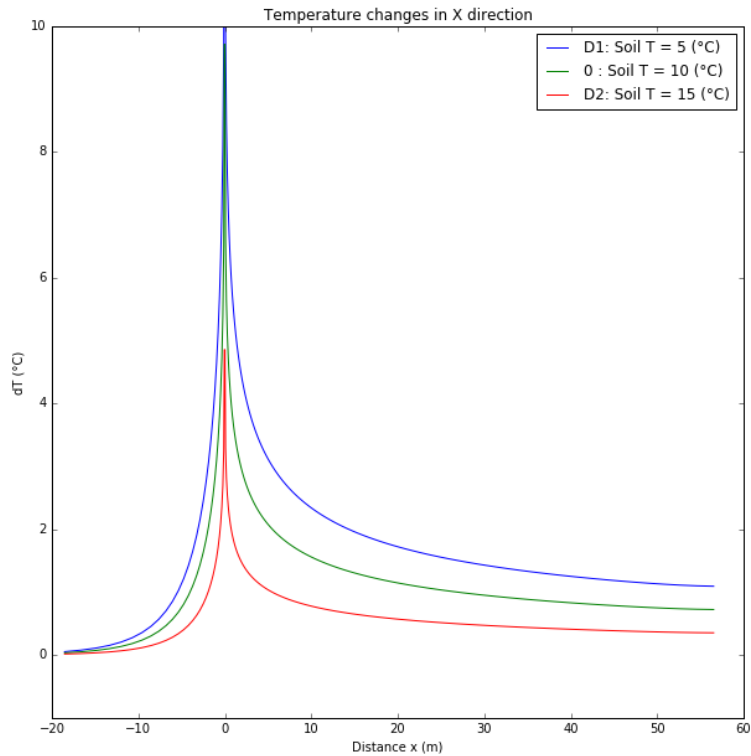


**Figure 24: Comparison of the distribution of soil temperature increase for different values of background soil temperature.**  
The cross section is crossing the bottom of the BTES system in the direction of groundwater flow.

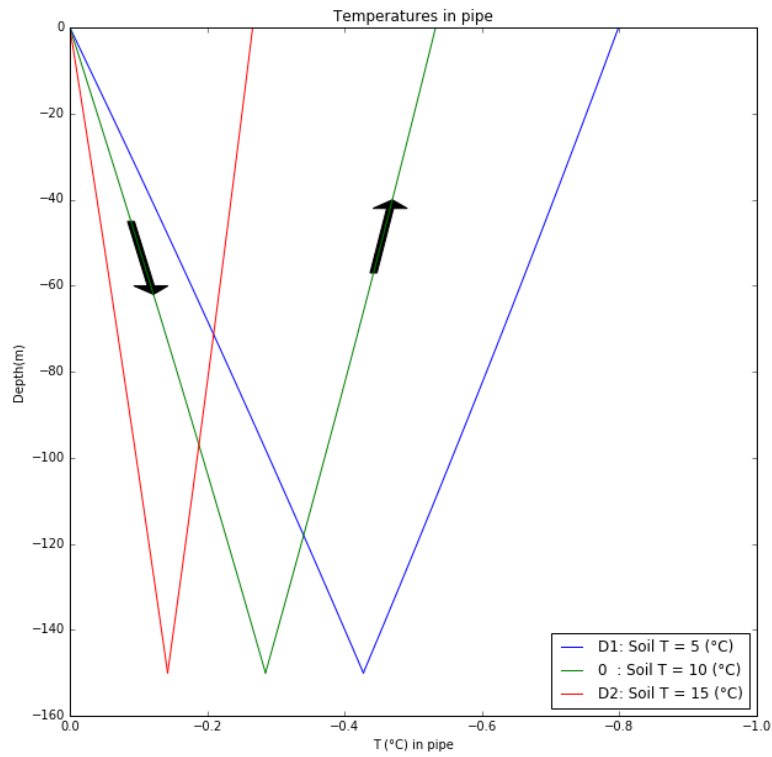


Figure 25: Comparison of the distribution of temperature decrease in the pipe for different levels of background soil temperature. Arrows indicate the direction of flow in the pipe.

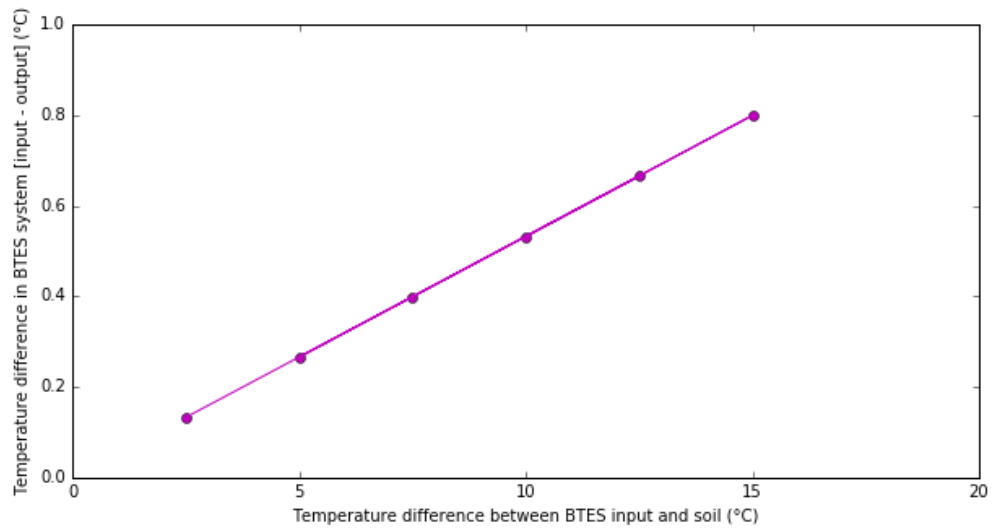


Figure 26: Relationship between output temperature difference of the pipe and background soil temperature

### *E. Pipe configuration*

Scenario E examines the effect of the pipe positioning, as depicted in Figure 17. In the reference case, the input and output points are positioned parallel to the direction of groundwater flow, with the output pipe downstream, while in this scenario the input and output points are reversed. In reality, it is hard to control the position of the pipes, as they usually become tangled when inserted in the borehole; in theory, however, it is interesting to check how the configuration of the system can affect the temperature exchange.

The outcome is presented in Table 8. As it can be seen both from the table and Figure 27 and 28, the change in the configuration has no effect at all in the temperature distribution and the stabilization time.

For tests conducted with much stronger groundwater flow, there was an interesting observation: even though the output temperature of the pipe is still not affected by the positioning, there is a deviation in the distribution of temperature along the pipe. When the pipe positioning is inverted, the largest part of the heat exchange takes place in the ascending part of the pipe (which is placed upstream), and the exchange on the descending part becomes lower, but overall the amount of heat disposed in the soil is almost equal for both cases.

**Table 8: Sensitivity analysis results for scenario E: Different pipe configuration**

Scenarios		0	E
Pipe configuration		0°	180°
dT downstream (°C)	10m	1.55	1.55
	30m	0.96	0.961
	50m	0.758	0.759
Stabilization time (years)		18.8	18.8
dT output (°C)		0.532	0.533
Energy flux (MJ /day)		230.86	231.29

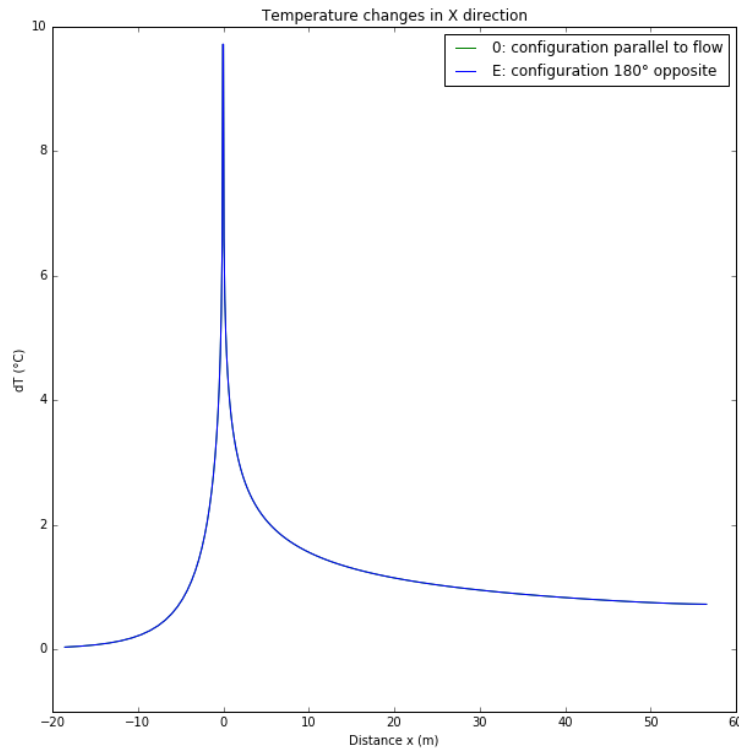


**Figure 27:** Comparison of the distribution of soil temperature increase for different configurations of the BTES system. The cross section is crossing the bottom of the BTES system in the direction of groundwater flow.

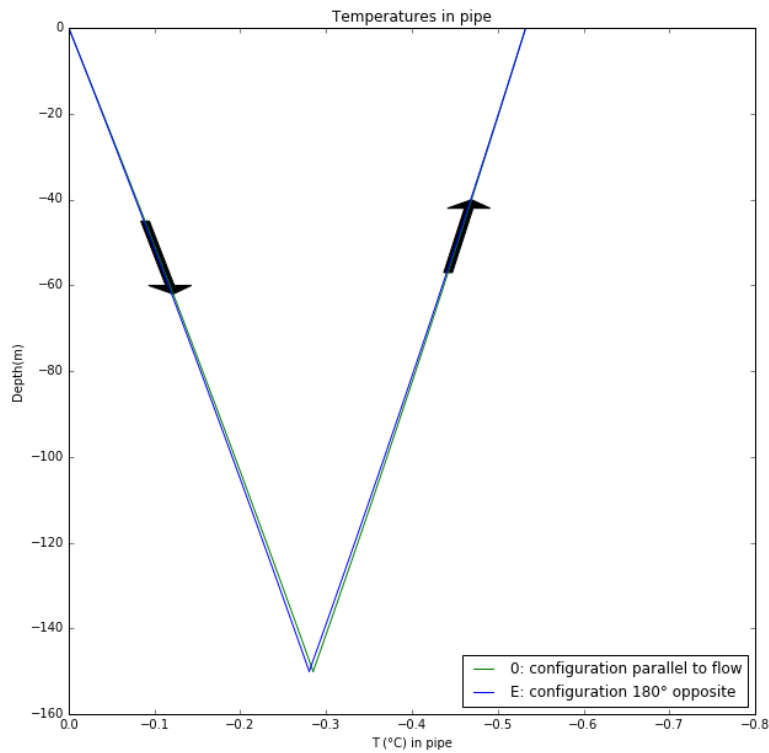


**Figure 28:** Comparison of the distribution of temperature decrease in the pipe for different configurations of the BTES pipe. Arrows indicate the direction of flow in the pipe.

### F. Soil layers with flow

In scenario 0, the whole length of the borehole is considered to be in an aquifer with uniform groundwater flow. In reality, it is more common for the BTES system to cross multiple soil layers with different flows, due to variations between different types of soil and the existence of impermeable layers. Scenarios F1 – F4 examine the effect of groundwater flow in different layers of the soil.

Table 9 shows the output of scenarios F1 – F4, compared with the initial scenario (groundwater flow in all layers) as well as scenario A0 (no groundwater flow). In this part of the sensitivity analysis, as the soil temperature distributions of each scenario vary with depth, they cannot be compared with each other; therefore the focus is only on the temperature and energy output of the BTES system.

**Table 9: Sensitivity analysis results for scenarios F1-F4 and A0: Different soil layers with flow**

Scenarios	0	F1	F2	F3	F4	A0
<b>Soil layers with flow</b>	<b>Everywhere</b>	<b>Top 50%</b>	<b>Bottom 50%</b>	<b>Top 30%</b>	<b>Bottom 60%</b>	<b>Nowhere</b>
dT output (°C)	0.532	0.49	0.49	0.449	0.499	0.452
Energy flux (MJ /day)	230.86	212.63	212.63	206.56	216.54	196.14

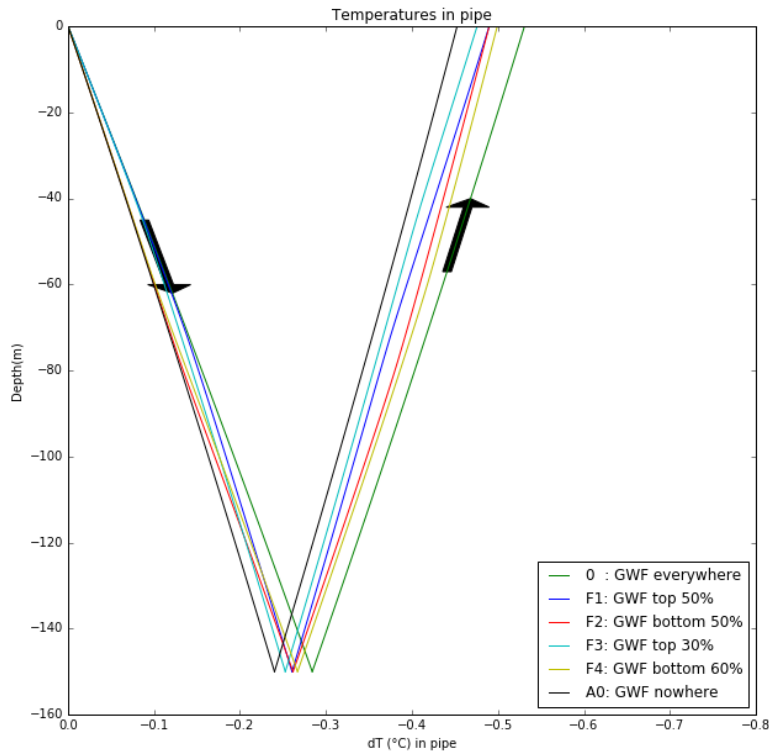


**Figure 29: Comparison of the distribution of temperature decrease in the pipe for cases of groundwater flow in different soil layers. Arrows indicate the direction of flow in the pipe.**

The results show that the output temperature and energy of the BTES system depends on the vertically integrated flow, and not on the depth at which flow is present. For scenarios F1 and F2, where flow is present around the top and bottom half of the borehole's length respectively, the distribution of temperature in the pipe differs (heat exchange is stronger in the soil layers where there is flow), but the overall temperature and energy output of the system is the same. For scenario F3, where there is flow only on the top 30% part of the soil, heat exchange is decreased compared to F1 and F2, while for scenario F4, where there is flow in the bottom 60% part, heat exchange is decreased.

The reason behind this seemingly proportionate relationship, is that the heat transfer rate per meter length of the pipe to the soil is almost constant. This means that the total heat transferred from the two pipes of the top half of the BTES, is almost equal to the total heat transferred from the two parts of the bottom half, which is why groundwater flow has the same effect on both parts. As it was illustrated in Figure 15, the heat transfer rate is in fact decreasing along the pipe, however the rate of decrease is small and barely distinguishable compared to the total heat transfer. If the heat transfer rate was more rapidly decreasing along the pipe, groundwater flow in the top layers would be expected to have a slightly larger effect on heat exchange compared to flow in the bottom layers; however, the effect of the soil layer is insignificant compared to the effect of the total groundwater discharge.

#### **G. Multiple BTES systems**

Even though the effect of groundwater flow on BTES performance has been studied, it most commonly concerns single BTES installations. There has been limited research on how much, and under what conditions, does groundwater flow affect the total efficiency of a system of multiple BTES systems (Dehkordi et al., 2015). These cases are much more complicated, as the boreholes interact with each other and heat transfer is affected differently in the upstream and downstream boreholes. Studying the effect of groundwater flow on multiple systems is out of the scope of this study; a case of 2 BTES systems is presented here to illustrate the complicated combined effect of groundwater flow and interaction between systems.

The second BTES system is identical to the first one (same size, input temperature and pipe flow rate) and is placed 10m downstream of the first one along the X axis. The resulting distribution of soil temperature increase compared with the initial scenario is illustrated in Figure 30 and 31 and the temperature decrease in the pipes is depicted in Figure 32.

It is clear that the influence of BTES 1 on BTES 2 is strong, while the reverse influence (BTES 2 on BTES 1) is negligible. Heat disposed by BTES 1 is carried with the groundwater flow towards BTES 2, causing the temperature of the soil around it to increase; for higher soil temperatures, heat transfer from the BTES system to the soil is decreased. Compared to the single BTES of scenario 0, the energy output of BTES 1 is only 2.1% lower, while the energy output of BTES 2 is 15.6% lower. As for the soil temperature distribution, it is increased by approximately 84% at all downstream points compared to the single BTES scenario.

**Table 10: Sensitivity analysis results for scenario G: Different number of BTES systems. The distances at which  $dT$  is computed for scenario G are with reference to the 2<sup>nd</sup> (downstream) BTES system.**

Scenarios		0	G
Number of BTES systems		One	Two
dT downstream (°C)	10 m	1.55	2.858
	30 m	0.96	1.771
	50 m	0.758	1.391
Stabilization time (years)		18.8	18
			BTES 1      BTES 2
dT output (°C)		0.532	0.521      0.449
Energy flux (MJ /day)		230.86	226.08      194.84

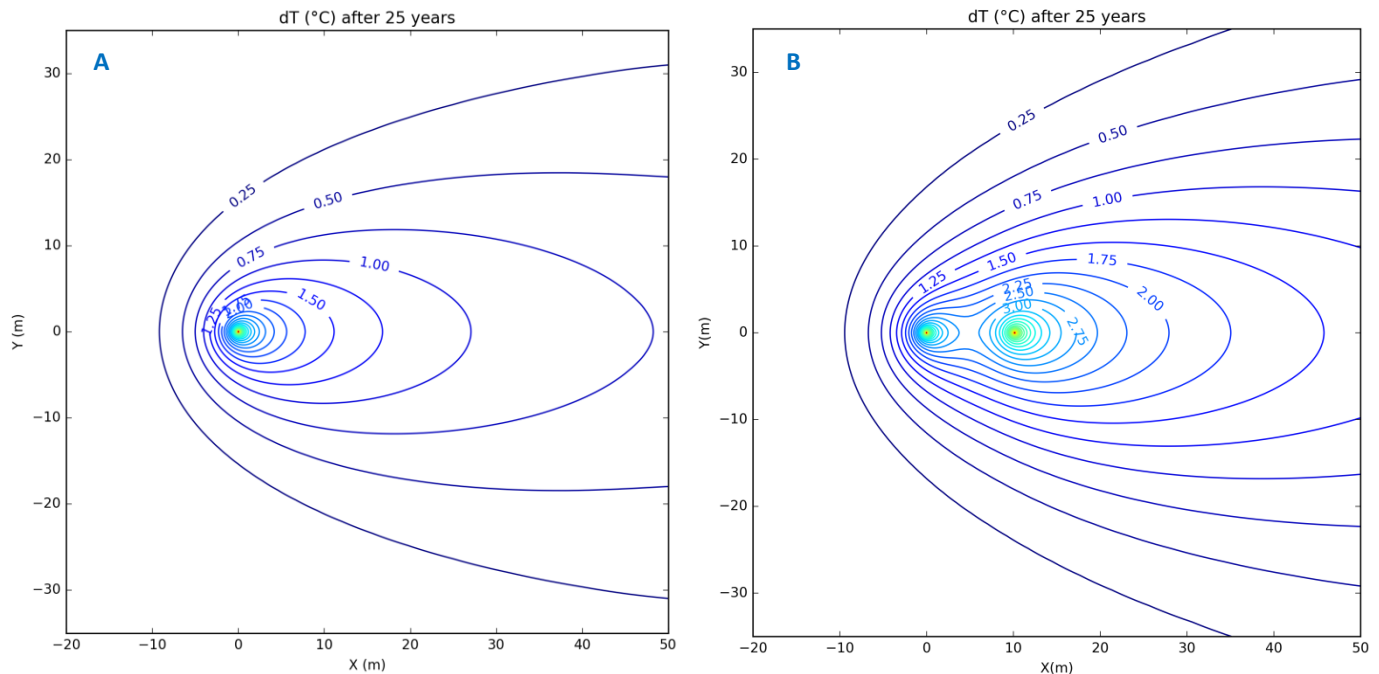


**Figure 30: Distribution of temperature change in the soil on a horizontal cross-section around the bottom of the borehole, after 25 years of constant operation of the systems. A: Scenario 0 (single BTES system). B: Scenario G: Two BTES systems placed at a distance of 10m from each other.**

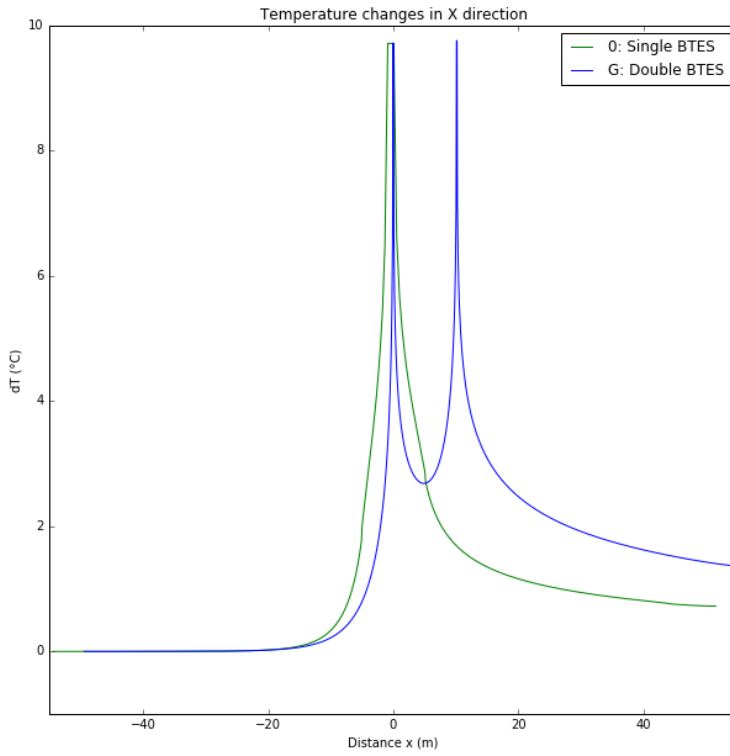


**Figure 31:** Comparison of the distribution of soil temperature increase in case of one or two BTES systems. The cross section is crossing the bottom of the BTES systems in the direction of groundwater flow.

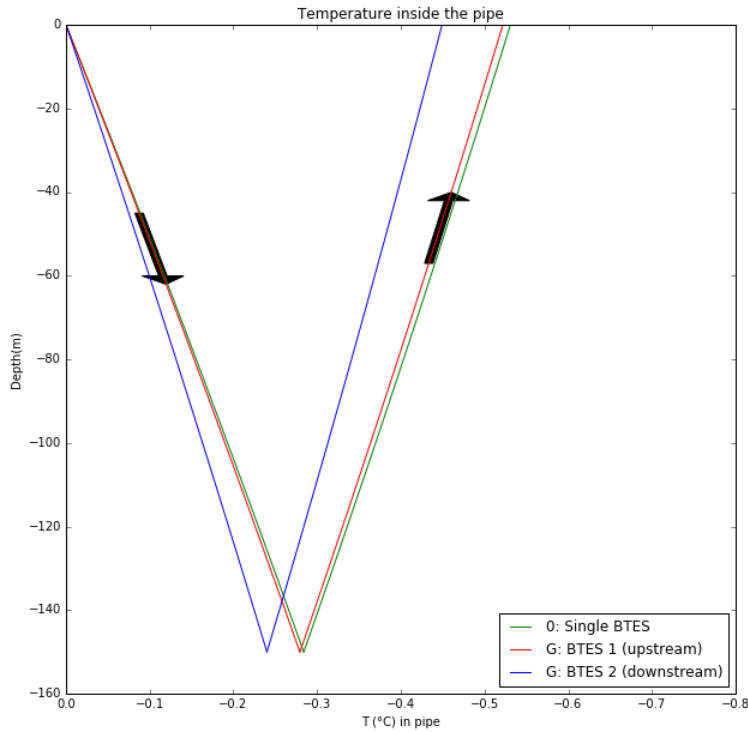


**Figure 32:** Comparison of the distribution of temperature decrease in the pipe in case of one or two BTES systems in the area. Arrows indicate the direction of flow in the pipe.

### 3.5. Conclusions

A model that simulates heat transfer between a BTES system and the subsurface under the effect of groundwater flow was developed in this chapter. The verification resulted in a good match between experiment and model, indicating that the model is reliable and can be applied to model real cases of BTES systems in areas with groundwater flow. The sensitivity analysis provides some useful insight on the parameters that affect the system's performance, which will help in calibrating the model to simulate a real case, and can be taken into account to design the installation of a system accordingly.

For a continuous heat injection with a constant input temperature for multiple years, the effect of groundwater flow on the distribution of heat in the soil downstream of the system is strong, but when the level of discharge is low, it takes a few years for the effect to become apparent. Groundwater flow enhances the system's heat exchange, as it helps in stabilizing the temperatures near the borehole and thus forming fixed temperature gradients between BTES and soil, resulting in a steady-state heat transfer rate. The system is sensitive to changes in the total groundwater discharge. The higher the level of groundwater flow, the higher the resulting heat transfer rate. The soil layer at which groundwater flow occurs, however (i.e. closer to the surface or to the bottom of the borehole), is insignificant. This is implied by comparing the outcomes of the sensitivity analysis on groundwater discharge (A) and on different soil layers with flow (F). Scenario A1 (where half of the discharge of the reference case is applied along the whole borehole length), and scenarios F1 and F2 (where the same groundwater discharge as the reference case is applied to 50% of the borehole length), all result in almost equal output temperatures and heat exchange rates. Even though these results might diverge in cases of larger heat exchange rates (and for variations of heat exchange rate along the pipe), it can be established as a rule of the thumb that the magnitude of the effect of groundwater flow on the heat exchange rate depends mainly on the total discharge of groundwater, and not on the soil layer in which it occurs.

Soil porosity has an adverse effect on the system's heat exchange; soils of low porosity are more favorable for BTES systems. In general, lower porosity enhances conduction (as it increases the thermal diffusivity coefficient D – eq. (3) ), as well as advection (as it increases the specific discharge – eq. (2) ), but it increases the retardation coefficient (eq. (4) ). This conflicting effect to the components of the heat transfer equation makes it complicated to assess the magnitude of porosity's effect on heat transfer, which differs depending on the level of groundwater flow, the temperature gradients and the thermal properties of the soil. Nevertheless, it is clearly revealed by the results that heat exchange between the BTES system and the ground is favored by low porosity.

The flow rate of the water circulating in the system has a strong effect on the resulting output temperatures; lower pipe flow rates result in higher temperature differences and vice versa, but the overall effect on the heat transfer rate is negligible. This result is useful for the calibration of the model; one of the reasons that decrease the accuracy of the model could be the velocity profile inside the pipe. In reality, water flows faster in the middle and slower near the walls of the pipe; this might allow the slower-flowing water near the walls to exchange more heat. In the finite-difference model, the cross-section of the pipe is modeled as one cell and the flow is averaged over that cell. Since the sensitivity analysis shows that the model output is highly sensitive to pipe flow velocity, this simplification could be

one of the reasons that the model underestimates the temperature difference compared to real systems.

The configuration of the inlet and outlet of the pipe with reference to the direction of the flow does not affect the heat exchange rate at all. As in reality the two parts of the pipe tend to twist, making it difficult to control their position inside the borehole, the fact that the positioning has no effect is useful information for the design process.

The sensitivity analysis reveals that soil temperature plays a very important role in heat exchange. This is clearly seen in the scenarios of different background soil temperature (D) and verified by the scenario of two BTES systems (G), where the soil temperature of the downstream system is increased due to advection of heat originating from the upstream system. It has been established that even for low levels of groundwater discharge, the downstream soil temperatures are affected in large distances from the system. It therefore becomes clear that the interaction between neighboring BTES system can be strongly intensified by groundwater flow. When both systems are operating in the same mode (heating/cooling), the heat exchange capacity of the downstream system is lowered.

## 4. Case study

### 4.1. Description of BTES system

In this chapter, a case study is built based on one of Itho-Daalderop's installed BTES systems. The system is located in the area of Bakel, east of Helmond and Eindhoven in the southern part of the Netherlands (Figure 33). The main criterion for choosing this location is the fact that the BTES system consists of a single vertical loop and is the only registered system in the area, therefore no interference from neighboring systems is expected.

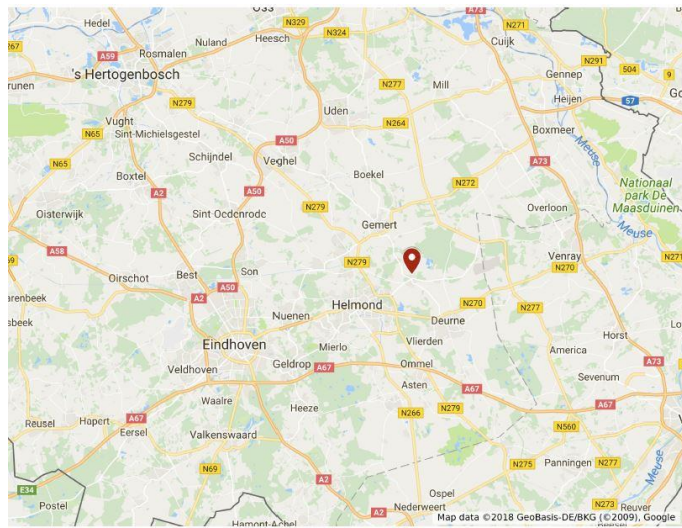


Figure 33: Location of the BTES case study system

Information on the subsurface can be found on DINOLoket ([www.dinoloket.nl](http://www.dinoloket.nl)). The subsurface in the area comprises different types of sandy soils. Due to privacy concerns, the exact coordinates of the system are not known, but an approximation can be made based on multiple similar soil profiles in the area. The depth is divided into four soil layers with different ranges of hydraulic conductivities – all relatively high. The values used for each layer were chosen within the given ranges after some calibration. For the thermal properties of the soil, uniform values estimated by Itho-Daalderop were applied to all layers. The background soil temperature was simulated as 10 °C, based on Itho-Daalderop's surface temperature measurement of 9.9 °C, after some calibration.

Table 11: BTES case study system design parameters

Borehole depth	90 m
Borehole diameter	0.15 m
Pipe (inner) diameter	26 mm
Spacing between inlet and outlet	0.06 m

The BTES system design parameters are listed in Table 11 and the hydraulic and thermal parameters of the soil, borehole filling material and water that are applied in the model are listed in Table 12. The BTES

is modeled in the middle of a  $110 \times 110 \text{ m}^2$  area, using the half-grid approach, as heads and temperatures are symmetrical with reference to the X-axis. The 90 m of depth are simulated using 30 layers of 3 m. Cell sizes vary from 6 cm in the borehole to 2 m at the boundaries, increasing on a logarithmic scale. The round pipe with a diameter of 26 mm is modeled as a square cell with a side of 23mm, which corresponds to an equal size of 530 mm<sup>2</sup>.

**Table 12: Model parameters and properties. The layers are numbered starting from the surface to the bottom of the borehole; the total thickness is 90m.**

Soil layer	Lithology <sup>(1)</sup>	Thickness <sup>(1)</sup>	K <sub>H</sub> <sup>(1)</sup>	K <sub>V</sub> <sup>(2)</sup>	n <sup>(3)</sup>	K <sub>s</sub> <sup>(4)</sup>	ρ <sub>s</sub> <sup>(4)</sup>	c <sub>s</sub> <sup>(4)</sup>
		m	m/day	m/day	(-)	W/m°C	kg/m <sup>3</sup>	J/m <sup>3</sup> °C
1	Sandy soil, mainly consisting of medium and fine sand	17	50	5	0.3	2.2	2650	906
2	Sandy soil, mainly consisting of coarse sand, gravel and medium sand	18	75	7.5	0.3	2.2	2650	906
3	Sandy soil, mainly consisting of coarse and medium sand	35	50	5	0.3	2.2	2650	906
4	Sandy soil, mainly consisting of medium, fine and coarse sand	20	10	1	0.3	2.2	2650	906
<b>Borehole filling material</b>						2	1700	1325
<b>Circulating fluid: water</b>						0.58	1000	4100

References: <sup>(1)</sup> Dinoloket <sup>(2)</sup>Assumed as  $0.1 \cdot K_H$  <sup>(3)</sup>geotechdata.info <sup>(4)</sup>Itho-Daalderop

An online tool developed by the Dutch Geological Service (Geologische Dienst Nederlands - [www.grondwatertools.nl](http://www.grondwatertools.nl)) was used to estimate groundwater flow. Based on a network of groundwater level measurements, the tool generates isohypsies maps which can be retrieved for specified areas and dates. Figure 34 illustrates the isohypsies map of the area around Bakel in December of 2017. The hydraulic head gradient in Bakel is estimated as  $1 - 2 \cdot 10^{-3}$  (ranging between 1 and 2 m of head difference over 1 km distance, depending on the exact location). An average gradient of  $1.5 \cdot 10^{-3}$  was applied to the simulation. Depending on the soil layer, this head gradient will induce groundwater flow with a (Darcy) velocity ranging between 0.45 – 3.4 m/month.

The boundary conditions are the same as in the main BTES model, described in 3.1: the north and south ends, as well as the top and bottom layers, are no-flow boundaries in MODFLOW and zero heat flux boundaries in MT3D; the east and west ends are constant head boundaries in MODFLOW and specified heat flux boundaries in MT3D.

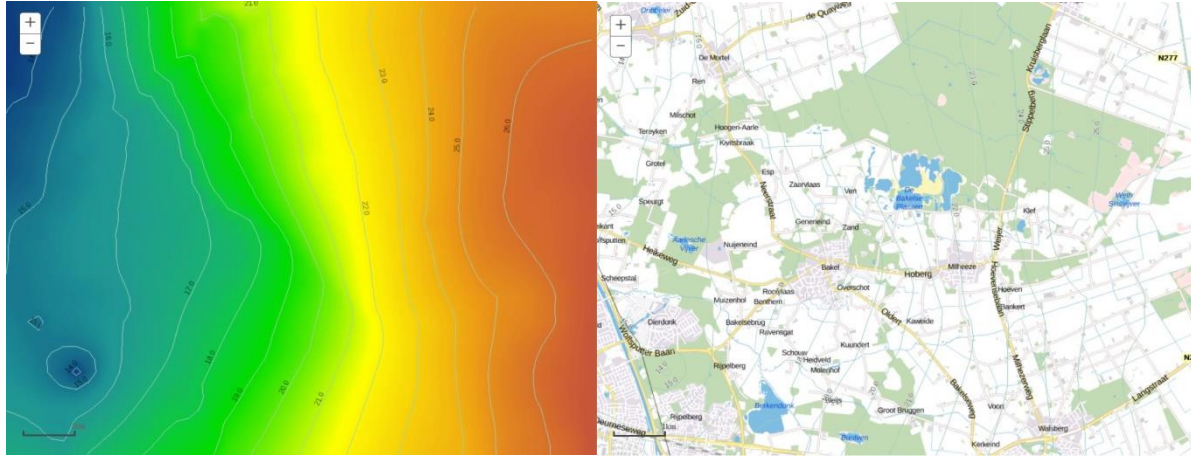


Figure 34: Isohypses map of the area around Bakel. Left: Filled isohypses contour lines. Right: Isohypses over map.

#### 4.2. Implementation of recorded dataset to the model

The BTES system has been active since June 2013, supplying the heating and cooling requirements of a small building. The pipe flow rates and input - output temperatures of the system are monitored by Itho-Daalderop and recorded for 2-hour time steps. A daily-averaged dataset of the system's operation over the last 12 months (May 2017 – May 2018) was used as input in the model.

The system is operating in cooling mode (storing heat in the ground) from May until the middle of September, and in heating mode (extracting heat) for the remaining time until May. The energy loads are therefore not balanced; the heating and cooling demand distribution in time is approximately 62% - 38%.

The results of the simulation, illustrated in Figure 35, show that the model underestimates the heat exchange for the most part of the simulation. The resulting difference between input and output temperatures of the model is approximately 60-70% of the measured difference, both in cooling and in heating mode. The modeled temperature difference is in the order of 2 °C throughout the simulation, while in reality it is in the order 3.5 °C.

There are a few uncertainties and assumptions involved in the model, making it complex to identify the cause of this underestimation. Based on the sensitivity analysis of the previous chapter, the porosity and background soil temperature – for which there was large uncertainty – were calibrated to match the measured results as much as possible. A low porosity of 0.3 was chosen in the end for all layers; for values lower than 0.3, the solver of MT3D would not converge. Changing the background soil temperature would not improve the results, as the system is operating in both heating and cooling modes. Lowering the soil temperature decreases the output temperatures of the system throughout the year, shifting the results closer to the measured dataset during heat injection, but increasing the gap during heat extraction – and vice versa for raising the soil temperature.

The hydraulic conductivities were chosen rather large within the ranges provided by DINOloket, resulting in groundwater discharge in the order of a few meters per month, which is rather fast. As it was already discussed in the previous chapter, higher groundwater discharge enhances the heat

injection rate; in this case study, it is pointed out that groundwater flow enhances the heat transfer rate in both heating and cooling modes. One possible explanation in this case for the lower performance of the model compared to the real system, could be that groundwater flow in the area is in fact stronger than it was indicated from the map of groundwater heads. If, for example, there are groundwater wells extracting water near the BTES location, strong groundwater flow would be induced, which would increase the heat exchange rate and the resulting  $\Delta T$  throughout the year.

Even though the model does not meet the real system's performance, it follows the same pattern in the fluctuations of output temperature and successfully predicts the peaks. It can therefore be used to simulate hypothetical scenarios to assess the effect of groundwater flow in the future; the scenario will drive the results to the same direction as in reality, but on a smaller scale.

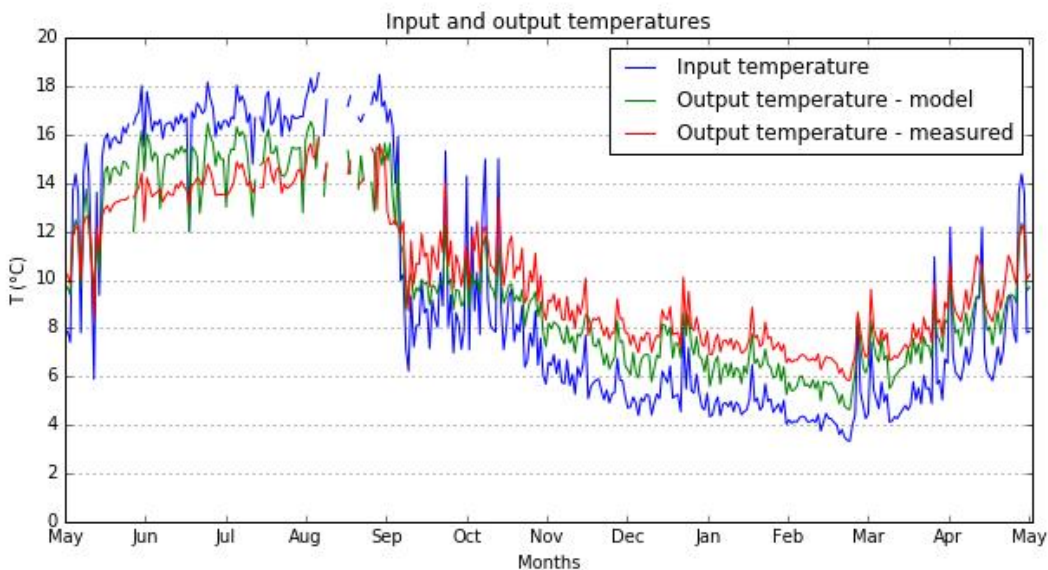


**Figure 35: Comparison of modeled and measured output temperatures and input temperatures of the BTES case study system. The gaps between August and September are short periods where no data was recorded.**

### 4.3. Scenarios

Based on the modeled case study, the given datasets are used to simulate the system's operation in the future for multiple consecutive years, comparing a scenario of high groundwater flow with a scenario of no groundwater flow. In the scenario with groundwater flow, the groundwater head gradient is increased to  $5 \cdot 10^{-3}$ , inducing steady-state groundwater flow with (Darcy) velocities ranging between 1.5 and 11.25 m/month, depending on the soil layer.

The given dataset of input temperatures is smoothed using the moving average technique on 60-days subsets, to make the pattern clearer. As a result, the transitional periods between the heating and cooling seasons – when the system is switched multiple times between the two modes within a month – are cleared out. The heat exchange pattern is averaged to 5 months of heat injection and 7 months of heat extraction per year.

The scenarios are implemented on the smoothed profile of input temperatures, repeated for three consecutive years. The results are illustrated in the graphs of Figures 36 – 39. Figure 36 shows the time periods when the system is switched to heating or cooling, as a reference point for the following graphs. Figure 37 compares the temperature difference between the input and output of the BTES pipe for the two scenarios. Figure 38 compares the heat extraction and injection rates between the two scenarios. Figure 39 compares the soil temperatures at four different points (one point upstream of the borehole, and three points downstream). The chosen points are all located at a depth of 30 m, in the second soil layer, where groundwater flow is maximized.

The figures reveal a pattern that is repeated each year, and that can be clearly distinguished in four phases.

- Phase 1 (May – October)

Phase 1 is the warm period, when heat is being injected to the ground. During this phase, heat transfer is enhanced by groundwater flow. Figure 37 shows higher temperature differences between the input and output of the pipe, and Figure 38 shows higher heat injection rates for the scenario with groundwater flow. By looking at Figure 39, it is observed that groundwater flow significantly lowers the temperatures in the vicinity of the borehole; in the downstream direction, the temperatures at a distance of 0.5 m (38-B) are more than 1°C lower compared with the scenario of no-flow, while at the same distance in the upstream direction (38-A), soil temperatures are almost constant at the initial soil temperature of 10°C. It is clear that during this phase, groundwater flow contributes beneficially to the system by carrying heat away from the borehole and allowing for more heat to be transferred to the soil.

- Phase 2 (October – November)

Phase 2 is the beginning of the cold season, which lasts for approximately one month after the system has been switched to heat extraction. During this phase, heat exchange is higher in the no-groundwater-flow scenario. The temperature changes of the water in the pipe in Figure 37 and the heat transfer rates in Figure 38 are larger when there is no groundwater flow, as the heat stored in the subsurface during phase 1 can now be extracted. In graphs A and B of Figure 39, we can see that the temperatures of the soil around the borehole are still colder in the scenario with groundwater flow; now that the system is in heat extraction mode, the gradients between BTES and ground temperatures are lower and thus hindering heat exchange.

- Phase 3 (December – April)

Phase 3 is the second part of the cold season. The system is still extracting heat, but the patterns between the two scenarios are now changing. The groundwater flow scenario results in higher heat extraction rates. During the heat extraction of phase 2, groundwater flow keeps the ground temperature near the borehole relatively stable, preventing it from dropping below a certain limit, as is revealed by Figure 39. When groundwater flow is absent, the ground keeps cooling down, becoming less and less beneficial for heat extraction.

- Phase 4 (April – May)

Phase 4 is the first month of the warm season, when the system is switched to heat injection again. It is not a part of the first cycle, and only appears from the second year onwards, as it is a result of the preceding cold season. During this month, the reverse effect of phase 2 takes place. In the case of no groundwater flow, the soil has been cooled down by the heat extraction, allowing for more heat to be injected by the system. In the case of groundwater flow, the soil temperature around the borehole is not as cold, as groundwater has kept it more stable; the soil therefore absorbs smaller amounts of heat.

Figure 38-B shows the difference between the absolute heat transfer rates of the two scenarios. The heat transfer rates are larger for the scenario with groundwater flow during phases 1 and 3, and they are only lower during the short phases 2 and 4 – it is easily observed that the total heat exchange of the system is much higher under the effect of groundwater flow.

From year to year, there is a slight change in the heat exchange pattern, which is not easily distinguished in the graphs. In the scenario where no groundwater flow occurs, the heat injection rate is increasing each year by 2-3 MJ/day, while the heat extraction rate is decreasing each year by approximately 1 MJ/day. In the scenario with groundwater flow, no change is observed in the yearly heat transfer rates.

Figure 39 shows the fluctuations of temperature in the subsurface. It is noticeable that just 2 m downstream from the borehole, the minimum and maximum peaks in temperature arrive one month earlier and are about 0.5°C higher in the case of groundwater flow, compared to the case of no groundwater flow. The result highlights the strong effect of groundwater flow on the downstream soil temperature distribution.

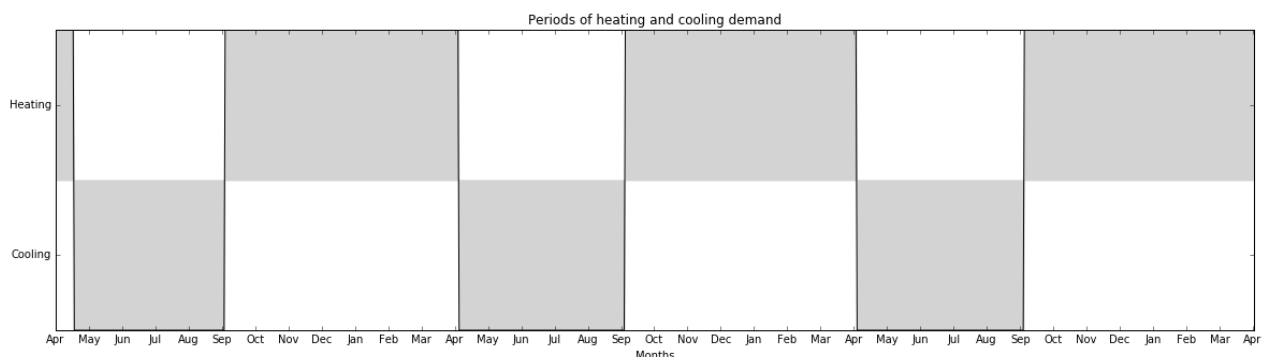


**Figure 36: Illustration of the heating - cooling demand profile; heating season corresponds to energy extraction from the subsurface, while cooling season corresponds to heat injection.**

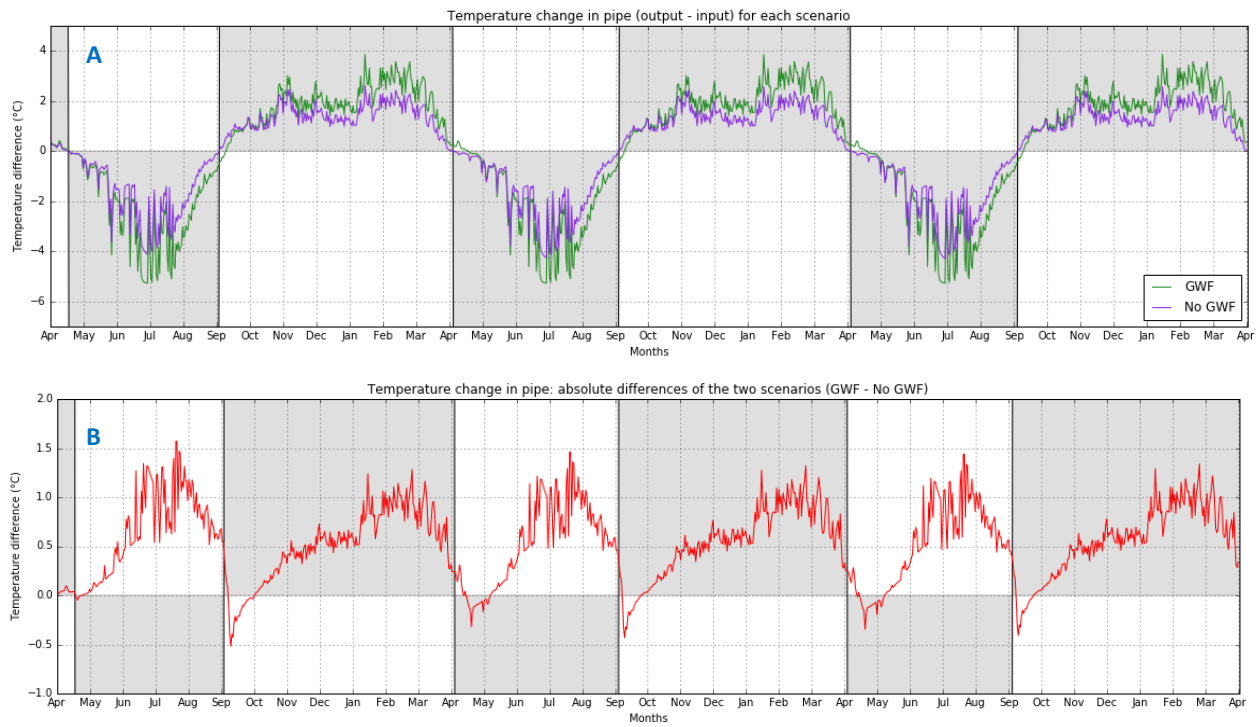


**Figure 37: Temperature differences between output and input of the BTES pipe, with and without groundwater flow.**  
**A:** Comparison of the two scenarios. Positive temperature difference indicates heat extraction. **B:** Subtraction of the scenarios from each other.

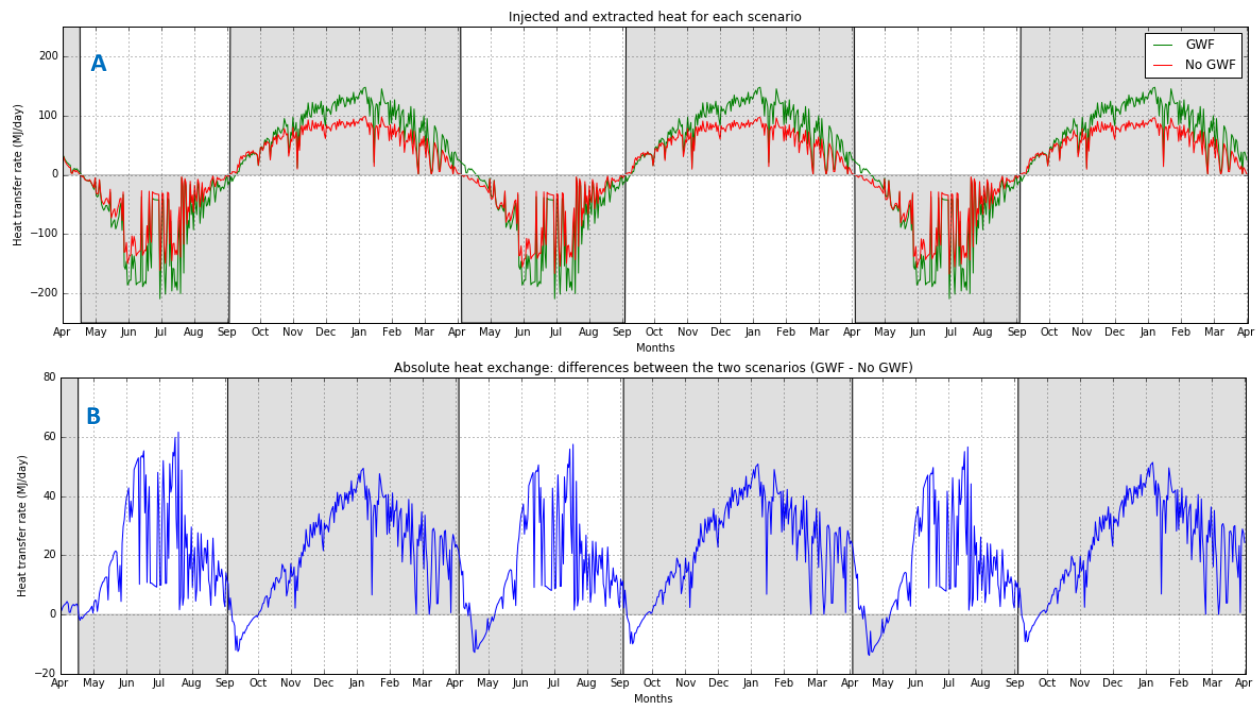


**Figure 38: Heat transfer rates of the BTES system, with and without groundwater flow.** **A:** Comparison of the two scenarios. Positive heat transfer rates indicate heat extraction. **B:** Differences in absolute energy transfer between the two scenarios.

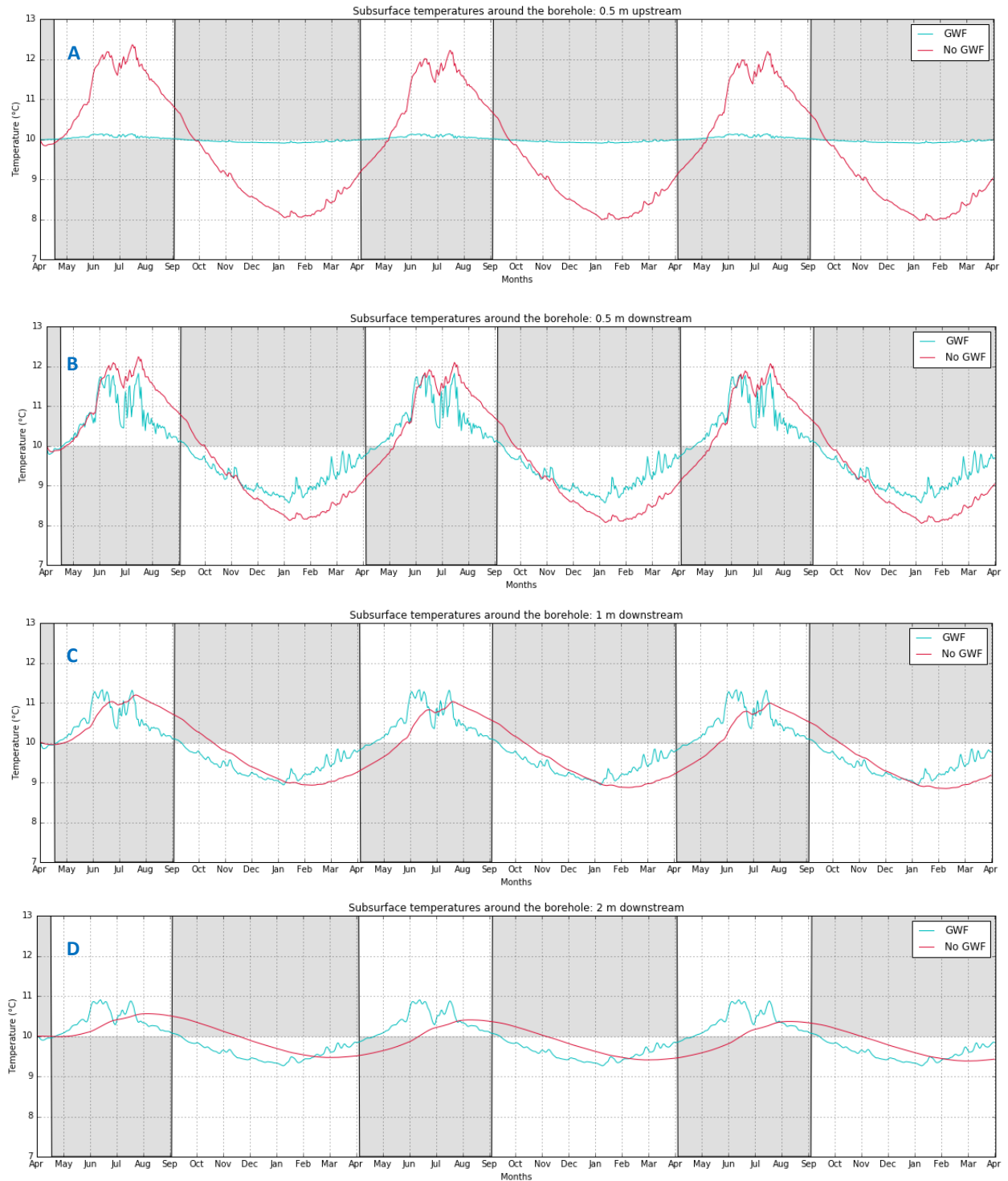


**Figure 39: Temperatures of the soil at selected points, located 30 m deep, with and without groundwater flow.**

#### **4.4. Discussion**

The results of the case study scenarios point out that groundwater flow has a clearly positive effect in the total heat exchange of a heating – cooling system. By observing the different phases of heat exchange, it is revealed that a BTES system under the effect of groundwater flow achieves lower heat transfer rates only during the short transitional periods between heating and cooling. During those periods, a system in an area with no groundwater flow is able to take advantage of the subsurface that has previously been heated up or cooled down, resulting in higher heat exchange rates. However, this incompetence of a system under groundwater flow to quickly adjust to shifts between heating and cooling mode, is subsequently overcompensated by the significantly higher heat exchange rates achieved as a result of the relatively stable temperatures of the subsurface around the borehole.

It has to be noted that, as a result of the moving average technique that was applied to the input temperatures dataset, the transitional periods between the two modes were smoothed out. In reality, during these periods, the system would switch between heating and cooling multiple times; this short-term heat storage and extraction is much more favorable for the scenario where no groundwater flow occurs, while in the groundwater flow scenario, the system is delivering much lower heat exchange rates. Even though this phenomenon can still be observed in the results, it is less intense, as a result of smoothing. In any case, however, the overall heat exchange in both heating and cooling modes is significantly higher in the case of groundwater flow.

It is observed that in the case where there is no groundwater flow, there is a small decrease in the heat extraction rate from year to year, and respectively an increase in the heat injection rate, while no such changes are observed in the case where groundwater flow occurs. This outcome indicates that for a long-term operation of the system with imbalanced energy demand (in this case, larger heat extraction), and without the influence of an external factor (e.g. heat fluxes from the surrounding area of the system), a net heat extraction is being accumulated in the lifetime of the system, gradually reducing the system's ability to extract heat. Groundwater flow contributes in dissipating the imbalanced energy loads, bringing the system to a steady-state heat exchange situation. This means that even for low values of groundwater flow, which would not have such a strong effect on the yearly heat exchange, there can be a positive impact on systems operating for multiple years under imbalanced energy loads.

## 5. Conclusions and recommendations

### 5.1. Conclusions and further research suggestions

The lack of simulation tools that can predict heat exchange between a BTES system and the subsurface, under the effect of both conduction and advection, has been stressed out in previous research (1.2). In this thesis, a tool suitable to reflect the effect of groundwater flow on the behavior a BTES system has been developed. The model has been verified with an analytical solution as well as experimental data, proving that it can be readily applied to predict the output temperatures of a BTES system in both heating and cooling modes, as well as the distribution of heat in the soil, under the effect of groundwater flow. The sensitivity analysis and the case study have offered important insight on the behavior of BTES systems under the effect of groundwater flow, which can prove helpful for the design of BTES systems in practice.

Groundwater flow contributes in forming relatively stable soil temperatures in the vicinity of the borehole. Regarding one-way heat transfer between the BTES system and the soil (i.e. only heat injection or only heat extraction), this stabilization of soil temperatures enhances heat exchange rates, as the temperature gradients that drive the heat transfer are kept above a certain limit. This effect is directly dependent on the magnitude of groundwater discharge – the higher the discharge, the higher the heat exchange rates. The soil layer at which groundwater flow occurs along the length of the borehole – closer to the surface or the bottom – does not play a significant role. Heat exchange is also highly dependent on porosity; less porous soils are more favorable for BTES systems.

In practice, it is difficult to measure groundwater discharge, therefore assessing its impact when designing a system can be challenging. However, when possible, it is recommended to estimate or measure the groundwater flow, as the required length of the heat exchangers can be reduced by taking the flow into account during design. It is also important to acquire accurate measurements of the background soil temperature and the porosities at different depths before installing a system, as these parameters have a significant effect on the heat transfer rates.

When it comes to systems that combine heating and cooling, the effect is more complex. In general, it has been revealed by the simulations that BTES systems under the effect of groundwater flow achieve lower heat exchange rates when switched from heating to cooling (and vice versa) on a daily scale, compared to cases where no groundwater flow is present, as heat is carried away from the borehole and cannot be extracted again. However, on a monthly scale, the stabilization of soil temperatures caused by high groundwater discharge proves to significantly increase the heat exchange rate, compared to cases where no groundwater flow occurs. In other words, in the short term, a large part of the stored heat can be extracted – therefore groundwater flow is not beneficial – but in the long term, the stored heat cannot be as efficiently extracted, and stable soil temperatures in the vicinity of the borehole are the main driver of the heat exchange – therefore groundwater flow becomes beneficial. The overall effect in cases of combined heating and cooling depends on the magnitude of the groundwater discharge, the magnitude and ratio of heating and cooling energy loads, and the frequency of switching between the two modes.

Regarding imbalanced heating and cooling loads, it is indicated that groundwater flow helps restore the soil's background temperature and counteract the imbalance, thus preventing a net heat extraction or injection from accumulating and possibly reducing the system's heat exchange capacity over the years. The length of BTES pipes often has to be over-designed to account for the long-term effect of energy load imbalance during the system's lifetime; groundwater flow therefore becomes an important design consideration, as it can compensate for the imbalanced loads and thus prevent this over-designing.

The results of the model tests and the case study highlight the importance of long-term simulations, as low groundwater flow can take multiple years before having a significant effect on the performance of the BTES system; however, long-term simulations include a high computational effort in terms of required time and memory, and were not feasible within the context of this project. As BTES is a relatively recent technology, further research should be conducted into the effect of groundwater flow after multiple years of operation of BTES systems.

Geothermal systems are becoming increasingly popular; the number of BTES systems installed in the Netherlands is estimated at 50.000 in 2015, with a growth of 5.000 every year(van Heekeren & Bakema, 2015). This means that by 2050, more than 200.000 systems will be installed in the country. This increase in the number of installations will inevitably lead to interaction between systems. It has been revealed in the simulations that even low discharges of groundwater flow affect the soil temperatures in long downstream distances from a BTES system, and the heat exchange rates of other BTES installations located downstream are significantly affected, as they are highly dependent on the background soil temperatures. More research should be conducted in the field, to gain better understanding of the effect of groundwater flow combined with mutual interaction between BTES systems.

## 5.2. Suggestions for model improvement

A powerful simulation tool has been created, which can be readily applied to predict the expected heat exchange of BTES systems as well as the soil temperatures in the vicinity of the systems. However, it has been noted that the model produces lower temperature differences between pipe input and output compared to real BTES systems. In this chapter, some recommendations on how the model can be improved are listed, for use in future research.

There are multiple reasons why the model has been found to underestimate the temperature difference in the pipe, mainly related to assumptions and simplifications. The simplifications were made in the initial version of the model, in order to keep it uncomplicated and thus have a better understanding of the results, as well as a clear view of the effect of each parameter in the sensitivity analysis; the more parametrized a model is, the more difficult it becomes to assess the effect of single parameters. For the verification of the method (3.3), as well as the simulation of the case study (4), more complex versions of the model was applied, using all the available information to bring the model as close to reality as possible. For example, the more complex versions included the borehole filling material and soil layers with different properties. These changes improved the matching of temperatures between the model outcome and the measured datasets, but there are still further suggestions on how to upgrade the model, in order to approach the full complexity of a real system as much as possible.

- The model assumes a uniform background soil temperature – in reality, the temperature profile in the top 15-20 m varies with depth and with time. As was demonstrated in the sensitivity analysis, the background soil temperature has a strong effect in the system output. A model that incorporates soil temperature varying with depth and with time in the top soil layers could yield output temperatures closer to real systems.
- The model uses the assumption of uniform thermal parameters. This was also applied in the case study, using the same (probably averaged) values provided by Itho-Daalderop's calculations in all the soil layers, as there was no data available on the thermal parameters of different soils. However, if variations in thermal conductivity and heat capacity values are available or can be determined, that could significantly improve the model's performance.
- The model does not account for the thermal properties and thickness of the pipe walls; it simulates heat transfer conducted directly from the circulating water to the ambient material (the soil, or the borehole filling material when included). Including a pipe material of high thermal conductivity in the simulation could increase the heat exchange.
- Thermal resistances of the materials have not been included in the simulation. The thermal resistance is the reciprocal of thermal conductance; it is a heat property that indicates the ability of a material to resist heat flow. The thermal resistances could be incorporated in the model by accordingly lowering the thermal conductivity values; this would not enhance the resulting heat exchange, but it is an important parameter that would make the simulation more precise.
- The simulated area is large, and the side boundaries are sufficiently far from the BTES system in all directions to not affect the heat transfer within this simulation time. However, the top and bottom layer boundaries are maybe not. Even though heat flux in the vertical direction was very low compared to the horizontal direction (as the borehole length is much longer compared to its diameter), it has to be noted that extending the bottom boundary to include the soil layers beneath the borehole could allow for vertical heat flux in the soil and perhaps enhance heat exchange between the soil and the BTES system.

## References

- Anderson, M. P. (2005). Heat as a ground water tracer. *Ground Water*, 43(6), 951–968.  
<https://doi.org/10.1111/j.1745-6584.2005.00052.x>
- Angelotti, A., Alberti, L., La Licata, I., & Antelmi, M. (2014). Borehole heat exchangers: Heat transfer simulation in the presence of a groundwater flow. *Journal of Physics: Conference Series*, 501(1).  
<https://doi.org/10.1088/1742-6596/501/1/012033>
- Bakema, G., & Schoof, F. (2016). Geothermal Energy Use, Country Update for The Netherlands. *European Geothermal Congress*.
- Bakker, M., Caljé, R., Schaars, F., van der Made, K.-J., & de Haas, S. (2015). An active heat tracer experiment to determine groundwater velocities using fiber optic cables installed with direct push equipment. *Water Resources Research*, 51(4), 2760–2772.  
<https://doi.org/10.1002/2014WR016632>
- Bakker, M., Post, V., Langevin, C. D., Hughes, J. D., White, J. T., Starn, J. J., & Fienen, M. N. (2016). Scripting MODFLOW Model Development Using Python and FloPy. *Groundwater*.  
<https://doi.org/10.1111/gwat.12413>
- Banks, D. (2012). An Introduction to Thermogeology: Ground Source Heating and Cooling. In *An Introduction to Thermogeology: Ground Source Heating and Cooling* (2nd ed.). Oxford, UK: Wiley-Blackwell. <https://doi.org/10.1002/9781118447512.ch1>
- Bauer, D., Heidemann, W., & Müller-Steinhagen, H. (2009). Modelling and simulation of groundwater influence on borehole thermal energy stores. In *Proceedings of Effstock, the 11th International Conference on Thermal Energy Storage*. Stockholm, Sweden: Stockholm International Fairs. Retrieved from [http://www.itw.uni-stuttgart.de/dokumente/Publikationen/publikationen\\_09-07.pdf](http://www.itw.uni-stuttgart.de/dokumente/Publikationen/publikationen_09-07.pdf)
- Bedekar, V., Morway, E. D., Langevin, C. D., & Tonkin, M. J. (2016). *MT3D-USGS version 1: A U.S. Geological Survey release of MT3DMS updated with new and expanded transport capabilities for use with MODFLOW - Techniques and Methods*. <https://doi.org/10.3133/tm6a53>
- Bruno, R., Mercuri, S., Tinti, F., & Witte, H. (2013). Probabilistic approach to TRT analysis : evaluation of groundwater flow effects and machine - borehole interaction. *European Geothermal Congress*, (June).
- Chiasson, A., Rees, S., & Spitler, J. (2000). A preliminary assessment of the effects of groundwater flow on closed-loop ground source heat pump systems. *ASHRAE Transactions*, 106(1), 380–393. Retrieved from <http://www.osti.gov/scitech/biblio/20104801>
- Dehkordi, S. E., Schincariol, R. A., & Olofsson, B. (2015). Impact of Groundwater Flow and Energy Load on Multiple Borehole Heat Exchangers. *Groundwater*, 53(4), 558–571.  
<https://doi.org/10.1111/gwat.12256>
- Diao, N., Li, Q., & Fang, Z. (2004). Heat transfer in ground heat exchangers with groundwater advection. *International Journal of Thermal Sciences*, 43(12), 1203–1211.

<https://doi.org/10.1016/J.IJTHERMALSCI.2004.04.009>

- Fuchs, S., Schütz, F., Förster, H.-J., & Förster, A. (2013). Evaluation of common mixing models for calculating bulk thermal conductivity of sedimentary rocks: Correction charts and new conversion equations. *Geothermics*, 47, 40–52. <https://doi.org/10.1016/j.geothermics.2013.02.002>
- Gehlin, S. E. A., & Hellström, G. (2003). Influence on thermal response test by groundwater flow in vertical fractures in hard rock. *Renewable Energy*, 28, 2221–2238. [https://doi.org/10.1016/S0960-1481\(03\)00128-9](https://doi.org/10.1016/S0960-1481(03)00128-9)
- Harbaugh, A. W. (2005). *MODFLOW-2005, The U.S. Geological Survey Modular Ground-Water Model—the Ground-Water Flow Process: U.S. Geological Survey - Techniques and Methods*. Retrieved from [http://inside.mines.edu/~epoeter/583CSM/DOC4\\_MODFLOW2005-TM6A16.pdf](http://inside.mines.edu/~epoeter/583CSM/DOC4_MODFLOW2005-TM6A16.pdf)
- Hecht-Méndez, J., Molina-Giraldo, N., Blum, P., & Bayer, P. (2010). Evaluating MT3DMS for heat transport simulation of closed geothermal systems. *Ground Water*, 48(5), 741–756. <https://doi.org/10.1111/j.1745-6584.2010.00678.x>
- Ingebritsen, S. E., & Sanford, W. E. (1998). *Groundwater in geologic processes*. Cambridge University Press.
- Ingersoll, L. R., Zobel, O. J., & Ingersoll, A. C. (1955). *Heat conduction with engineering, geological and other applications*. Thames and Hudson (Vol. 81). London: John Wiley & Sons, Ltd. <https://doi.org/10.1002/qj.49708135036>
- Johansen, O. (1977). *Thermal conductivity of soils*. Corps of Engineers, U.S. Army, Cold Regions Research and Engineering Laboratory, Hanover, N.H.
- Kelvin, W. T., Larmor, J., & Joule, J. P. (1882). *Mathematical and physical papers*. Cambridge, University Press.
- Langevin, C. D., Thorne, D. T. J., Dausman, A. M., Sukop, M. C., & Weixing, G. (2008). *SEAWAT Version 4: A Computer Program for Simulation of Multi-Species Solute and Heat Transport. Techniques and Methods, Book 6, Chapter A22*.
- Pellenbarg, N. P. (1997). Groundwater management in the Netherlands: Background and legislation groundwater in the Netherlands. In A. Schrevel (Ed.), *ILRI Workshop: Groundwater Management: Sharing responsibility for an open access resource* (pp. pp137-149). Wageningen. Retrieved from [http://content.alterra.wur.nl/Internet/webdocs/ilri-publicaties/special\\_reports/Srep9/Srep9.pdf](http://content.alterra.wur.nl/Internet/webdocs/ilri-publicaties/special_reports/Srep9/Srep9.pdf)
- REA - Renewable Energy Association. (n.d.). Retrieved March 23, 2018, from <https://www.r-e-a.net/>
- Ren, T., Kluitenberg, G. J., & Horton, R. (2000). Determining Soil Water Flux and Pore Water Velocity by a Heat Pulse Technique. *Soil Science Society of America Journal*, 64(2), 552. <https://doi.org/10.2136/sssaj2000.642552x>
- Richards, M. L. (2017). *Ground coupled heat pumps: An analysis of their sustainability*. Delft University of Technology.
- Soilpedia. (n.d.). Retrieved March 23, 2018, from <https://soilpedia.nl/Bikiwiki afbeeldingen/Bodem en energie/WKO.jpg>

- Su, D., Diao, N., & Fang, Z. (2004). An analytical solution of the temperature response in ground heat exchangers with groundwater advection. In *6th International Symposium on Heat Transfer* (pp. 362–366). Beijing, China.
- Thorne, D., Langevin, C. D., & Sukop, M. C. (2006). Addition of simultaneous heat and solute transport and variable fluid viscosity to SEAWAT. *Computers and Geosciences*, 32(10), 1758–1768.  
<https://doi.org/10.1016/j.cageo.2006.04.005>
- van Heekeren, V., & Bakema, G. (2015). The Netherlands Country Update on Geothermal Energy. *Proceedings World Geothermal Congress 2015, Melbourne, Australia, 19-25 April, 2013*(April), 2–7.
- Witte, H. J. L. (2012). Error Analysis of Thermal Response Tests. *Innstock*, 1–20.
- Witte, H. J. L., & van Gelder, A. J. (2006). Geothermal response tests using controlled multi-power level heating and cooling pulses (MPL-HCP): Quantifying groundwater effects on heat transport around a borehole heat exchanger.
- Woodside, W., & Messmer, J. H. (1961). Thermal Conductivity of Porous Media. I. Unconsolidated Sands. *Journal of Applied Physics*, 32(9), 1688–1699. <https://doi.org/10.1063/1.1728419>
- Zheng, C., & Wang, P. P. (1999). *A Modular Three-Dimensional Multispecies Transport Model for Simulation of Advection, Dispersion and Chemical Reactions of Contaminants in Groundwater Systems: Documentation and User's Guide*. Retrieved from <http://www.geology.wisc.edu/courses/g727/mt3dmanual.pdf>

#### Websites

<http://www.groenholland.com/>

<http://www.ithodaalderop.nl/>

<https://www.grondwatertools.nl/grondwatertools-viewer>

<https://www.dinoloket.nl/>

<http://www.geotechdata.info/>